



## Article

# Activation of $\beta$ 2-Adrenergic Receptors in Microglia Alleviates Neuropathic Hypersensitivity in Mice

Elisa Damo <sup>1</sup>, Amit Agarwal <sup>2,3</sup> and Manuela Simonetti <sup>1,\*</sup>

<sup>1</sup> Institute of Pharmacology, Medical Faculty Heidelberg, Heidelberg University, Im Neuenheimer Feld 366, 69120 Heidelberg, Germany

<sup>2</sup> The Chica and Heinz Schaller Research Group, Institute of Anatomy and Cell Biology, Heidelberg University, Im Neuenheimer Feld 307, 69120 Heidelberg, Germany

<sup>3</sup> Interdisciplinary Center for Neurosciences, Heidelberg University, Im Neuenheimer Feld 366, 69120 Heidelberg, Germany

\* Correspondence: manuela.simonetti@pharma.uni-heidelberg.de

**Abstract:** Drugs enhancing the availability of noradrenaline are gaining prominence in the therapy of chronic neuropathic pain. However, underlying mechanisms are not well understood, and research has thus far focused on  $\alpha$ 2-adrenergic receptors and neuronal excitability. Adrenergic receptors are also expressed on glial cells, but their roles toward antinociception are not well deciphered. This study addresses the contribution of  $\beta$ 2-adrenergic receptors ( $\beta$ 2-ARs) to the therapeutic modulation of neuropathic pain in mice. We report that selective activation of  $\beta$ 2-ARs with Formoterol inhibits pro-inflammatory signaling in microglia *ex vivo* and nerve injury-induced structural remodeling and functional activation of microglia *in vivo*. Systemic delivery of Formoterol inhibits behaviors related to neuropathic pain, such as mechanical hypersensitivity, cold allodynia as well as the aversive component of pain, and reverses chronically established neuropathic pain. Using conditional gene targeting for microglia-specific deletion of  $\beta$ 2-ARs, we demonstrate that the anti-allodynic effects of Formoterol are primarily mediated by microglia. Although Formoterol also reduces astrogliosis at late stages of neuropathic pain, these functions are unrelated to  $\beta$ 2-AR signaling in microglia. Our results underline the value of developing microglial  $\beta$ 2-AR agonists for relief from neuropathic pain and clarify mechanistic underpinnings.



**Citation:** Damo, E.; Agarwal, A.; Simonetti, M. Activation of  $\beta$ 2-Adrenergic Receptors in Microglia Alleviates Neuropathic Hypersensitivity in Mice. *Cells* **2023**, *12*, 284. <https://doi.org/10.3390/cells12020284>

Academic Editor: Valerio Magnaghi

Received: 1 November 2022

Revised: 22 December 2022

Accepted: 8 January 2023

Published: 11 January 2023



**Copyright:** © 2023 by the authors. Licensee MDPI, Basel, Switzerland. This article is an open access article distributed under the terms and conditions of the Creative Commons Attribution (CC BY) license (<https://creativecommons.org/licenses/by/4.0/>).

**Keywords:** neuropathic pain; spared nerve injury; microglia; astrocytes;  $\beta$ 2-adrenergic receptor; pain-associated behavior

## 1. Introduction

Chronic pain is one of the most common health problems worldwide. About seven to eight percent of the adult population suffers from chronic pain of neuropathic origin, i.e., resulting from diseases or syndromes affecting the somatosensory system or from direct nerve damage [1]. Although several analgesic drugs are available, a large proportion of patients do not respond satisfactorily to traditional treatments. Although, opioids show adequate efficacy, after a short period of treatment they lead to tolerance and strong side effects [1]. Hence, it is essential to study the molecular mechanisms of neuropathic pain to identify new molecular targets, which can be capitalized on the development of new therapies for pain relief.

Antidepressant drugs, which enhance the synaptic availability of serotonin (5-HT) and noradrenaline (NA), have emerged as key therapeutics in neuropathic pain. Several studies reported that serotonin noradrenaline reuptake inhibitors (SNRIs), a class of antidepressants, are particularly effective in treating neuropathic pain that is refractory to other treatments [1,2], and their actions are mainly driven by enhancing NA availability [3]. NA is known to modulate pain both peripherally, where it is released by sympathetic neurons, or centrally, where it is released in the spinal dorsal horn from axons of the

bulbospinal descending noradrenergic pathway originating in the locus coeruleus (LC). At the molecular level, the analgesic effect of NA has been suggested to be mediated by activation of the  $\alpha$ 2a-adrenergic receptor ( $\alpha$ 2a-AR), a Gi-coupled receptor, which activation blocks neuronal activity [4]. Similarly, 5-HT and NA released from descending pathways promote the spinal release of enkephalins, which also exert neuronal inhibition through the activation of Gi-coupled opioid receptors [5]. In addition, activation of Gi-coupled receptors leads to the inhibition of glutamate release from primary afferent fibers as well as to the hyperpolarization of postsynaptic neurons in the dorsal horn of the spinal cord, inhibiting voltage-gated  $\text{Ca}^{2+}$  channels and opening inward rectifying  $\text{K}^{+}$  channels, respectively [6]. Activation of  $\alpha$ 2a-AR in the dorsal horn prevents neuroinflammatory changes associated with rodent models of chronic pain, reducing the release of inflammatory cytokines [7].

While efforts thus far have focused on adrenergic signaling in neurons, it is becoming increasingly evident that glial cells, including the two main central glial classes of astrocytes and microglia, express a variety of adrenergic receptors [8,9]. In particular, astrocytes and microglia express high levels of  $\alpha$ 2a-AR and  $\beta$ 2-AR, respectively, two receptor families known to play a role in neuropathic pain [10]. So far, however, the role of adrenergic signaling in glia in chronic pain has not been thoroughly explored.

The essential contribution of glial cells in the regulation of neural plasticity in pathways of nociception and pain is well-documented [11,12], and glial cells have emerged to be a crucial element in the development and maintenance of chronic pain [13]. Spinally, astrocytes and microglia are proposed to be activated in a consequential manner in various models of inflammatory and neuropathic origin [12,14,15]. Interfering with their activation at an early stage can block the development of nociceptive hypersensitivity [12], whereas optogenetic activation of astrocytes in the spinal cord has been shown to be sufficient to cause nociceptive hypersensitivity [16]. Following peripheral neuronal damage, primary afferents release various substances such as the colony-stimulating factor 1 (CSF-1) [17] and cytokines in the spinal cord, which bind to specific receptors on microglia and activate them [18]. The activated microglia in turn produce a wide variety of active substances that act on neurons and astrocytes, initiating a crosstalk that has been suggested to sustain chronic changes in nociceptive sensitivity.

While  $\alpha$ 2-ARs have been at the center of studies addressing adrenergic modulation of pain for decades, recent research has focused on the  $\beta$ 2-ARs. Systemic administration of  $\beta$ 2-AR agonists has been shown to have anti-inflammatory and anti-nociceptive properties in long-lasting inflammatory pain [19,20], neuropathic pain [21] and incisional pain [22]. Microglia express high levels of Gs-coupled  $\beta$ 2-AR [23,24] and respond to the application of NA [9,25–28]. However, given the broad distribution of  $\beta$ 2-AR in neurons, astrocytes, microglia and a variety of non-neuronal cells, the role of microglial  $\beta$ 2-AR signaling remains unknown.

We designed this study to delineate the contribution of microglia to the analgesic actions of  $\beta$ 2-AR agonists in rodent models of neuropathic pain, with emphasis on both sensory and emotional components of pain. A further goal was to study the underlying cellular and molecular mechanisms. Importantly, given the complex interplay between spinal neurons, microglia and astrocytes following nerve injury, we sought to pinpoint the temporal phases of pathophysiology induced by nerve injury in which targeting  $\beta$ 2-AR in microglia would bring maximum benefits. Employing highly specific genetic tools, we demonstrate the key significance of adrenergic signaling in microglia via  $\beta$ 2-AR in molecular plasticity in the spinal cord and ensuing neuropathic pain. Our findings underscore a major therapeutic potential for targeting microglial  $\beta$ 2-AR in neuropathic pain and yield key scientific insights into the neurobiological underpinnings of neuropathic pain.

## 2. Materials and Methods

### 2.1. Animal Handling

All experimental procedures were approved by the local governing body (Regierungspräsidium Karlsruhe, Germany, Ref. 35-9185.81/G-177/17 and 35-9185.81/G-274/19) and

abided by German laws that regulate animal welfare and the protection of animals used for a scientific purpose (TierSchG, TierSchVersV).

C57BL/6J mice (WT mice) of both sexes were purchased from Janvier Labs (Le Genest Saint Isle, Mayenne, France). Adult mice (8 weeks old, 20–30 g) were used for behavioral, qPCR, and immunofluorescence experiments, while 5-week old C57BL/6J mice were utilized for microglia primary cell culture.

To generate mice lacking  $\beta$ 2-AR specifically in microglial cells, mice carrying a conditional allele for the *Adrb2* (*Adrb2<sup>fl/fl</sup>*) gene (shared by Dr. Gerald Karsenty (Columbia University, New York, NY, USA)) [29], were crossed with inducible *Cx3cr1-CreERT2* mice (shared by Dr. Steffen Jung (The Weizmann Institute of Science, Rehovot, Israel), and Dr. Frank Kirchhoff (Center for Integrative Physiology and Molecular Medicine, University of Saarland, Homburg, Germany)) [30] that express the tamoxifen-inducible Cre under control of microglia and macrophages specific promoter. Cre-mediated recombination of *Adrb2* floxed allele was induced in 5-week old *Cx3cr1-CreERT2; Adrb2<sup>fl/fl</sup>* mice by injecting intraperitoneally (i.p.) 50 mg/kg Tamoxifen (10 mg/mL, cat # T5648 Sigma-Aldrich/Merck, Darmstadt, Germany) once per day over 5 consecutive days. To ensure a complete loss of function of *Adrb2* protein in microglial cells, we waited for three weeks after tamoxifen treatment before proceeding with the experiments. Adult *Cx3cr1-CreERT2; Adrb2<sup>-/-</sup>*; mice (8–9 weeks old) were used for behavioral and immunohistochemistry experiments.

A total of 258 C57BL/6J mice (130 males and 128 females), 100 *Cx3cr1-CreERT2; Adrb2<sup>fl/fl</sup>* mice (50 males and 50 females) were used for the experiments.

Mice of the same sex were housed together in groups of 2–4 per cage and kept under a 12 h light/dark cycle at controlled temperature ( $22 \pm 2$  °C), humidity (50–60%) with food and water provided ad libitum in conformity with ARRIVE guidelines.

## 2.2. Surgical Procedures and Nerve Injury

Mice of both sexes were assigned randomly and equally to spared nerve injury (SNI) or sham groups. SNI operation was performed according to earlier protocols [31] with minor modifications. Briefly, 8–9-week-old male and female mice were anesthetized using a mix of 2% isoflurane, oxygen and nitrous oxide. The common peroneal and tibial nerves were exposed via an incision of the lateral thigh skin, tightly ligated and cut distally. A 1 mm section was removed from the ligation leaving the sural nerve intact. The sham operation proceeded similarly without any nerve damage. The muscle tissue was restored, and the skin was stitched with Marlin 4-0 absorbable suture.

## 2.3. Pharmacological Drugs

Mice were i.p. injected with 50  $\mu$ g/kg of Formoterol (cat # 1448, Tocris, Wiesbaden-Nordenstadt, Germany) [32] or its solvent (0.9% NaCl) 1 h before behavioral analysis or perfusion for immunofluorescence experiments.

## 2.4. Behavioral Tests

Animals were randomly assigned into different groups. All behavior tests were performed double-blinded, which complied with the guidelines of the International Association for the Study of Pain. The experimenter was thus unaware of the identity of the treatment groups. All behavioral measurements were performed in awake, unrestrained, age and sex-matched adult mice.

### 2.4.1. Experimental Design

Basal measurements for mechanical and cold hypersensitivity were taken twice, once per day, two days before the SNI or sham operation using von Frey filaments and cold plate test, respectively. The cold plate test was performed sequentially after the von Frey filament test. Mechanical hypersensitivity and cold plate tests were performed following three different experimental plans:

- (i) The first one assessed the behavioral response of the mice on day three after the operation, one hour after receiving i.p. 50 µg/kg of Formoterol or saline.
- (ii) In the second paradigm, we tested mechanical and cold hypersensitivity six and 21 days after the operation, each day 1 h after injecting i.p. Formoterol or saline.
- (iii) In the third experimental scheme, we evaluated behavioral parameters only on day 21 after the surgery, one hour after receiving i.p. Formoterol or saline.

To analyze the mechanical and thermal (cold) response over time after the Formoterol injection, von Frey filaments measurements were taken 1, 6, 12 and 24 h after the Formoterol injection. For each time point, we tested each group of mice first with mechanical test and then with thermal test. Because of the technical time required to perform the mechanical tests (about 2 h), the thermal tests were performed with some delay from drug injection. This resulted in each group being tested for mechanical stimuli 1, 6, 12 and 24 h after injection, while thermal tests were performed 3, 8, 14 and 26 h after injection.

In order to avoid undue stress to the animals, we used a different cohort of mice to test the missing time points for each test (3 h for the mechanical test and 1 h for the thermal test; these time points are shown in a separate graph (Figure S1C,D) to reduce the time interval between the different recordings and not to lose an early potential analgesic effect.

The conditioned place preference (CPP) experiment was started on day 4 (Figure S2B) and day 32 (Figure S2D) after the sham or SNI operation with male and female mice as described below.

#### 2.4.2. Mechanical Sensitivity

Mice were habituated to the experimental setup, the von Frey elevated grid (Ugo Basile Inc., Gemonio (VA), Italy), for 1 h in three separate sessions within the week preceding the time of behavioral testing as well as 20–30 min before each testing session. Mechanical sensitivity testing was performed on an elevated grid by applying a set of von Frey filaments with increasing forces (0.008–1.0 g) to the affected and the contralateral hind paws using the up-down method described by Dixon [33]. Withdrawal frequencies were determined from 5 applications per filament, with a minimal interval of 5 min between filaments. Paw lifting and licking were defined as positive responses. The 50% withdrawal threshold (g) was determined by fitting the response rate vs. von Frey force curves with a Boltzmann sigmoid equation with constant bottom and top constraints equal to 0 and 100, respectively [34]. The integral of response frequency–von Frey force intensity (0.008 to 0.1 g) curves was calculated as area under the curve (AUC, A.U. = arbitrary unit).

#### 2.4.3. Cold Allodynia

Following the mechanical sensitivity test, animals were placed on a rectangular cold metal surface (4 °C, Hot/Cold Plate 35100, Ugo Basile Inc., Italy) enclosed by a Perspex cylinder, and closely monitored to record the latency of the first nociceptive response (paw lifting, shaking, licking, or jumping). A 30 s cut-off was used to prevent potential injury to the paws. Measurements were repeated at least three times during each test session.

#### 2.4.4. Conditioned Place Preference Test

The CPP test was used to determine the ability of Formoterol in exerting pain relief from ongoing pain, as described previously [35]. Test mice were conditioned to associate one of the two compartments with pain relief. Behavioral testing was performed between 9:00 a.m. and 4:00 p.m. in the 9-week-old mice and every session lasted 30 min. Baseline preferences were detected before the conditioning by placing the mice on the setup and letting them freely move between the chambers. Conditioning started one day after the baseline detection. Each day for three days, the mice were injected first with saline and after 10 min they were inserted in the assigned chamber. After at least 4 h from the saline injection, the mice were injected with Formoterol and 50 min later they were placed in the other chamber. The day after conditioning, the mice were placed on the setup and let to move freely across the chambers. The CPP sessions were video-recorded and scored

using ANY-maze (Stoelting Europe, Churchtown, Dublin, Ireland, ANY-maze 7.1) for the time spent in the two compartments. The change in time spent in the Formoterol chamber, referred to as score, is calculated as the difference in time spent in the Formoterol-associated chamber on the baseline and test day.

### 2.5. Immunohistochemistry, Imaging, and Cell Counting

At 3, 6 and 21 days from the operation and 1 h after Formoterol or saline i.p. injection, mice were perfused transcardially with cold PBS followed by 4% PFA. The spinal column was collected and post-fixed at 4 °C overnight in 4% PFA. The day after, the L3–L4 spinal segment was extracted, cryopreserved overnight in 30% sucrose, and cryosectioned at 20 µm. Sections were stored at –20 °C.

Immunostaining was performed according to the standard protocols for immunofluorescence staining [36]. Briefly, sections were washed in PBS, incubated for 15 min in 50 mM Glycine, and blocked for 1 h in blocking solution (10% normal horse serum in PBS). The following antibodies were incubated at 4 °C overnight: rabbit-anti-Iba1 (1:500, cat # 019-19741, Wako, Osaka, Japan), chicken-anti-Iba1 (1:500, cat # 234 009, Synaptic System, Göttingen, Germany), rabbit-anti-p-p38 (1:300, cat # 9212, Cell Signaling Technology, Leiden, The Netherlands), mouse-anti-p-JNK (1:200, cat # 9255, Cell Signaling Technology), rabbit-anti-p-JNK (1:100, cat # 4668, Cell Signaling Technology), guinea pig-anti-GFAP (1:1000, cat # 173 004, Synaptic System). Negative controls were incubated overnight in blocking solution. On the following day, sections were washed for 15 min in blocking solution and 15 min in PBST (PBS buffer plus TX-100). Successively, the secondary antibodies donkey anti-chicken Alexa 488-conjugated antibody (1:1000, cat # A78948 ThermoFisher Scientific Invitrogen, Darmstadt, Germany), donkey anti-mouse Alexa 488-conjugated antibody (1:1000, cat # A32766 ThermoFisher Scientific Invitrogen), donkey anti-rabbit Alexa 594-conjugated antibody (1:1000, cat # A21207, ThermoFisher Scientific Invitrogen), and goat anti-guinea pig Alexa 647-conjugated antibody (1:1000, cat # A11076 ThermoFisher Scientific Invitrogen) diluted in blocking solution were incubated for 1 h. Sections were washed three times for 10 min in blocking solution, treated with Hoechst 33342 (cat # H3570 ThermoFisher Scientific) diluted 1:10000 in PBS for 15 min, and rinsed two times for 10 min in PBST. Lastly, the sections were incubated for 10 min in 10 mM TRIS/HCl before mounting them on glass slides with Mowiol (cat # 0713.1 Carl Roth, Karlsruhe, Germany) and stored at 4 °C.

For p-JNK detection, slides were incubated for 20 min into an antigen retrieval buffer (10 mM of sodium citrate, 0.05% Tween 20, pH 6) at 80 °C in the water bath. After cooling for 30 min at room temperature, sections were washed once in 1 × PBS for 5 min followed by the standard protocol. Labeled slices were imaged using identical illumination exposure parameters for all animals with a confocal laser-scanning microscope (20×, 40× objectives: TCS SP8 AOBS, Leica, Wetzlar, Germany). Sequential line scans were used for spinal cord sections. A montage of confocal image stacks was acquired over a depth of 12 µm. For morphological analysis of microglia, slices were imaged with an epifluorescence microscope (40× objective: Nikon Y-TV55, Düsseldorf, Germany) using identical illumination exposure parameters for all groups. Images were taken with a total depth of 5 µm. The maximum z-projection spinal cord images were applied to be evaluated via Fiji-Image J software (version 1.52p, National Institutes of Health (NIH), Bethesda, Maryland, USA).

Counting was carried out in the contra and ipsilateral spinal dorsal horn (SDH), lamina I-II-III on 3–6 sections on each side across the entire region of interest. In these regions, we counted the number of Iba1-positive cells and double-positive p-p38/Iba1, p-JNK/Iba1, and p-JNK/GFAP cells. Fiji-Image J cell counter plug-in was used. For fluorescence intensity detection of GFAP, the region of interest was drawn and calculated as the mean grey value. The results were then divided by the area to have the intensity density per area unit. Data are expressed as the ratio between the ipsilateral and contralateral sides. For morphological analysis, 15–20 cells were analyzed per mouse. The microglial soma perimeter and the process length were assessed employing Fiji-Image J.

## 2.6. Microglia Isolation

For cell culture experiments, the entire spinal cords of 5-week-old mice were processed. For RNA extraction the L3–L5 lumbar part of the SDHs of three 8-week-old mice were employed and pulled together for each condition. Microglia isolation was performed using the gentle MACS Dissociator (Miltenyi Biotec, Bergisch Gladbach, Germany). Briefly, spinal cord tissues were homogenized using the Adult Brain Dissociation Kit (mouse and rat, cat # 130-107-677, Miltenyi Biotec) and running the gentleMACS program 37C\_ABDK\_02 following the manufacturer's instructions.

The resulting cell suspension, when used for RNA extraction, was subjected to treatment with the Myelin Removal Beads II (cat # 130-096-731, Miltenyi Biotec) adjusting the volume of the buffer and the beads according to the amount of initial tissue, whereas when used for the cell culture this step was avoided. Subsequently, the cells were incubated with CD11b Microbeads (1:10, cat # 130-049-601, Miltenyi Biotec) and microglia were isolated using a magnetic MACS separator. Sorted microglia were harvested for further cell culture or stored at  $-80\text{ }^{\circ}\text{C}$  for quantitative PCR. A purity check was obtained by RT-PCR investigating specific gene markers for neurons (*Syt1 V2*), astrocytes (*Aqp4*), oligodendrocytes (*Mbp*), and microglia (*Cx3cr1*) (Table 1). Primer efficiency: 1.96 (*Cx3cr1*), 1.98 (*Aqp4*), 2.01 (*Syt1 V2*), 2.07 (*Mbp*).

**Table 1.** Primers used for RT-PCR to check the purity of sorted microglia.

Primer	Sequence 5' → 3' Forward	Sequence 5' → 3' Reverse
<i>Syt1 V2</i>	CTCAACTGGCATTGTGTTAGTCAA	AGACTGCGGATGTTGGTGTG
<i>Aqp4</i>	TGGAGGATTGGGAGTCACC	TGAACACCAACTGGAAAGTGA
<i>Mbp</i>	ATTGGGTCGCCATGGGAAAC	CCAGCCTCTCCTCGGTGAAT
<i>Cx3cr1</i>	CGTGAGACTGGGTGAGTGAC	GGACATGGTGAGGTCCTGAG

## 2.7. Cell Culture

Sorted microglia were resuspended in cell culture medium, plated on a poly-D-Lysine (cat # P6407-5MG Sigma-Aldrich/Merck) coated glass coverslip in a 24 well/plate, and grown at  $37\text{ }^{\circ}\text{C}$  under 5%  $\text{CO}_2$  in the incubator. The cell culture medium consists of DMEM medium (cat # 11995-065, ThermoFisher Scientific) supplemented with Penicillin-Streptomycin (cat # 15140-122, ThermoFisher Scientific), G-5 Supplement (1:100, cat # 17503012, ThermoFisher Scientific), IL-34 (100 ng/mL, cat # 200-34, Peprotech, Hamburg, Germany), cholesterol (1.5 g/mL, cat # C3045, Sigma-Aldrich/Merck), TGF- $\beta$ 2 (2 ng/mL, cat # 100-35B, Peprotech), following the protocol from Bohlen et al. [37]. During the first five days in culture, CSF-1 (10 ng/mL, cat # 300-25, Peprotech) was added to promote cell survival and proliferation. Since CSF-1 induces an activated state of microglia cells, the primary cultures were kept for another five days in the culture medium without CSF-1 to let the cells acquire a resting phenotype, or with CSF-1 to mimic the neuropathic condition (activated microglia).

## 2.8. Dot Blot

Primary microglia cells from C57Bl/6 J mice cultured in the presence of CSF-1 were treated with Formoterol (10 ng/mL, cat # 1448, Tocris) or a vehicle for 1 h. The supernatant was quickly collected, frozen and kept at  $-80\text{ }^{\circ}\text{C}$ . Collected supernatants were used to analyze the released inflammatory mediators using the Mouse Inflammation Antibody Array, Membrane 40 Targets (cat # ab133999, Abcam, Berlin, Germany) following the manufacturer's instruction.

## 2.9. RNA Extraction and qPCR

L3-L5 SDH tissue and microglia from the L3-L5 SDH were quickly collected and snap-frozen on dry ice. After extracting the total RNA using the TRIzol method (cat # 15596018), a purification treatment with Deoxyribonuclease I Amplification Grade (cat # 18068-015)

was employed as per the manufacturer's instructions. The first-strand cDNA synthesis was retrotranscribed using 1 µg of total RNA, oligo(dT)20 primers (cat # 18418020), random hexamer (cat # N8080127), and SuperScript III Reverse Transcriptase (cat # 18080044) according to the manufacturer's instructions. As a control reverse, transcriptase was omitted. All the reagents used for RNA extraction, purification and first-strand cDNA synthesis were from ThermoFisher Scientific.

Quantitative PCRs were run using qPCRBIO SyGreen mix separate-Rox (cat # PB20.14-51 PCRBIO SYSTEMS) and specific primers (Tables 1 and 2) or *Gapdh* as housekeeping gene (Sigma-Aldrich/Merck), on a LightCycler 96 Real-Time PCR System (Roche, Basel, Switzerland). The data were analyzed using the related software. The expression level of the target mRNA was normalized to the expression of *Gapdh* mRNA. The relative gene expression was quantified using the comparative  $\Delta\Delta C_t$  method. Primer efficiency: 1.96 (*Adrb2*), 1.98 (*Gapdh*).

**Table 2.** Primers used for RT-PCR to study spinal cord expression of adrenoceptors.

Primer	Sequence 5' → 3' Forward	Sequence 5' → 3' Reverse
<i>Adrb2</i>	GCATGGAAGGCTTTGTGAAC	CTTGGGAGTCAACGCTAAGG
<i>Gapdh</i>	AGAAGGTGGTGAAGCAGGCATC	CGAAGGTGGAAGAGTGGGAGTTG

### 2.10. Statistical Analysis

All data are expressed as mean  $\pm$  standard error of the mean (SEM). Statistical analysis was performed using Prism 9 (GraphPad Software, LLC, San Diego, CA, USA, GraphPad Prism 9.4.1). When comparing two groups of data two-tailed, an unpaired Student's *t*-test was used, whereas when multiple groups and variables were compared, two-way ANOVA was employed and a post-hoc Tukey's test for multiple comparisons was performed to determine statistically significant differences.

A *p*-value of <0.05 was considered significant. Sample number (*n*), *p*-values, and interactions (when the two-way ANOVA test was utilized) are indicated in the figure legends.

### 2.11. Data Availability

The authors agree to make all raw data available and will upload raw data to a repository of Heidelberg University which is currently under construction. Furthermore, the raw data of this study will be made available on a request to M.S. (manuela.simonetti@pharma.uni-heidelberg.de).

## 3. Results

### 3.1. $\beta$ 2-ARs Are Upregulated in Spinal Microglia Early after Nerve Injury and Their Activation Attenuates Inflammatory Mediators in Microglia

Because activation of the noradrenergic descending pathway has been suggested to regulate neuroimmune processes, we addressed whether microglia are affected and whether  $\beta$ 2-ARs play a role. Therefore, we isolated microglia from segment L3-L5 of the SDH of wild-type mice using the magnetic-assisted cell sorting (MACS) technique. Next, we ascertained the purity of microglia extraction through quantitative RT-PCR (qPCR) analysis, which revealed enrichment of the microglial gene and a lack of expression of genes expressed in neurons (*Syt1 V2*), astrocytes (*Aqp4*) and oligodendrocytes (*Mbp*) (Figure 1A).

To study whether nerve injury changes the expression of the murine gene encoding  $\beta$ 2-ARs (*Adrb2*), we employed the spared nerve injury (SNI) model of neuropathic pain or sham surgery as a control. Three days post-surgery, we extracted mRNA from MACS-sorted microglia or total spinal cord lysates from L3-L5 of SDH. Using qPCR, we examined the expression of *Adrb2* in SNI and sham conditions, while the *Adrb2* expression did not differ significantly in bulk mRNA isolated from SDH samples (Figure S1A), we observed a significant and robust upregulation of *Adrb2* in microglia isolated from L3-L5 of SDH from mice with SNI compared to sham-operated mice (Figure 1B). Thus, we conclude

that the expression of *Adrb2* is specifically upregulated in spinal cord microglia early after nerve injury.

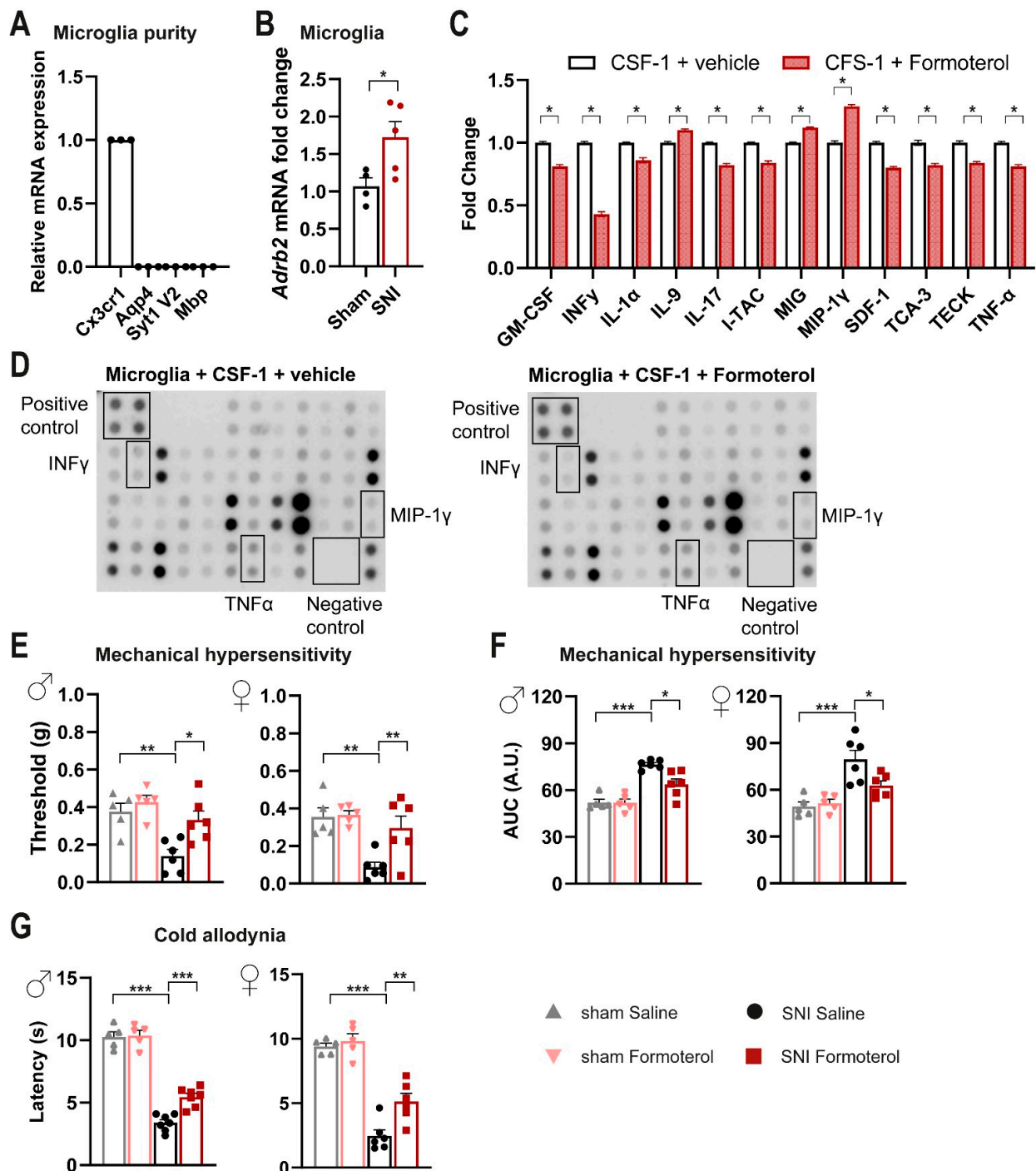


**Figure 1.** Spared nerve injury-induced induces upregulation of the *Adrb2* mRNA in microglia, whereas  $\beta$ 2-AR agonist decreases inflammation markers in activated primary microglia cell culture and sensitization in vivo. (A) Purity check of microglia isolated from the spinal dorsal horn via qPCR on markers specific for microglia (*Cx3cr1*), astrocytes (*Aqp4*), neurons (*Syt1 V2*), and oligodendrocytes (*Mbp*).  $n = 3$ . (B) Relative expression of *Adrb2* mRNA in microglia isolated from the spinal dorsal horn of SNI- and sham-operated mice three days after surgery.  $n = 4-5$ /group; two-tailed unpaired  $t$ -test was performed;  $* p < 0.05$  as compared between two groups. (C) Activated cultured microglia decrease the release of inflammatory mediators after Formoterol treatment.  $n = 4$ ; two-tailed



unpaired *t*-test was performed; \*  $p < 0.05$  as compared between two groups. (D) Examples of dot blots for inflammatory cytokines released from activated primary microglia culture (CSF-1 treated) after vehicle or Formoterol treatment. (E,F) Behavioral analysis of the effects of intraperitoneal Formoterol administration on mechanical sensitivity measured 1 h after intraperitoneal injection of Formoterol (E) in male (left,  $F_{1, 18} = 3.35$ ,  $p = 0.0659$ ) and female (right,  $F_{1, 18} = 6.184$ ,  $p = 0.0229$ ) mice. Integral of response frequency–von Frey force intensity (0.008 to 0.1 g) curves (AUC, A.U. = arbitrary unit) (F) three days after SNI or sham operation, using male (left;  $F_{1, 20} = 3.169$ ;  $p = 0.0903$ ) and female (right;  $F_{1, 18} = 5.561$ ,  $p = 0.0299$ ) mice. (G) Cold allodynia measured after Formoterol injection, three days after operation, using mice of both genders (male:  $F_{1, 20} = 8.808$ ,  $p = 0.0076$ ; female:  $F_{1, 18} = 4.913$ ,  $p = 0.0398$ ).  $n = 5\text{--}7/\text{group}$ ; two-way ANOVA test; \*  $p < 0.05$ , \*\*  $p < 0.01$ , \*\*\*  $p < 0.001$ . Data are expressed as mean  $\pm$  SEM, individual data points are displayed.

Furthermore, we generated primary microglia cultures from the spinal cord tissue of wild-type mice. To emulate microglial activation post-nerve injury, we incubated cultured microglia with CSF-1 [17] and tested the impact of treatment with the  $\beta_2$ -AR specific agonist Formoterol or the corresponding vehicle. We found that Formoterol treatment attenuated the CSF-1-induced expression of inflammatory mediators such as interleukin 1 alpha (IL-1 $\alpha$ ), interferon-gamma (INF- $\gamma$ ), tumor necrosis factor-alpha (TNF- $\alpha$ ), and interleukin 17 (IL-17) (Figure 1C,D), compared to the vehicle. Moreover, the level of chemokines that induce proliferation and/or promote chemotaxis of immune cells to the injury site (granulocyte-macrophage colony-stimulating factor (GM-CSF), interferon-inducible T cell alpha chemoattractant (I-TAC), stromal cell-derived factor 1 (SDF-1), chemokine ligand 1 (TCA-3/CCL1) and chemokine ligand 25 (TECK/CCL25)) also decreased. Expression of anti-inflammatory cytokines such as interleukin 9 (IL-9) increased in the Formoterol-treated cultures, as well as other chemotactic cytokines for migrating immune cells such as macrophage inflammatory protein-1 gamma (MIP-1 $\gamma$ /CCL9) and monokine induced by interferon-gamma (MIG) (Figure 1C,D). Thus, activation of  $\beta_2$ -ARs in microglia suppresses pro-inflammatory signaling and the response of microglia.

### 3.2. Impact of In Vivo Administration of $\beta_2$ -AR Agonist on Mechanical and Cold Hypersensitivity in Mice over Early Stages Post-Nerve Injury

Formoterol has been previously reported to exert an anti-nociceptive effect in a neuropathic pain model [32], but its mechanism is not yet clarified. We chose to apply Formoterol systemically via intraperitoneal (i.p.) delivery to facilitate therapeutic relevance and studied its anti-nociceptive effect in the SNI model of neuropathic pain. Three days post-SNI, a detailed time-course analysis of behavioral responses to mechanical and cold stimuli showed that the maximum inhibitory effect on mechanical hyperalgesia is reached 1 h after Formoterol injection, whereas peak inhibition of cold hypersensitivity occurs at 3 h (Figure S1C,D). In both male and female mice, Formoterol injection significantly reduced SNI-induced mechanical hypersensitivity, compared to saline-treated SNI mice (Figure 1E,F; the integral of the response frequency-von Frey stimulus intensity curve from 0.008 to 1.0 g is shown). Moreover, in both genders, Formoterol application significantly increased the latency of paw withdrawal after cold stimuli compared with SNI-operated vehicle-treated mice, indicating a reduction in SNI-induced cold allodynia (i.e., when non-noxious cold is perceived as noxious) (Figure 1G). These results thus indicate that systemic delivery of a  $\beta_2$ -AR agonist attenuates mechanical and cold hypersensitivity over the early stages of post-nerve injury.

### 3.3. Formoterol Reverses Hypersensitivity Established over Several Days to Weeks and Alleviates Spontaneous Pain in Mice Post-SNI

Our analyses at early stages post-SNI (Figure 1E–G) uncovered the potential of systemically applied Formoterol in inhibiting the development of nociceptive hypersensitivity to mechanical and cold stimuli. Thus, we tested the impact of Formoterol in reversing hypersensitivity once it is established over several days to weeks (Figure 2A).

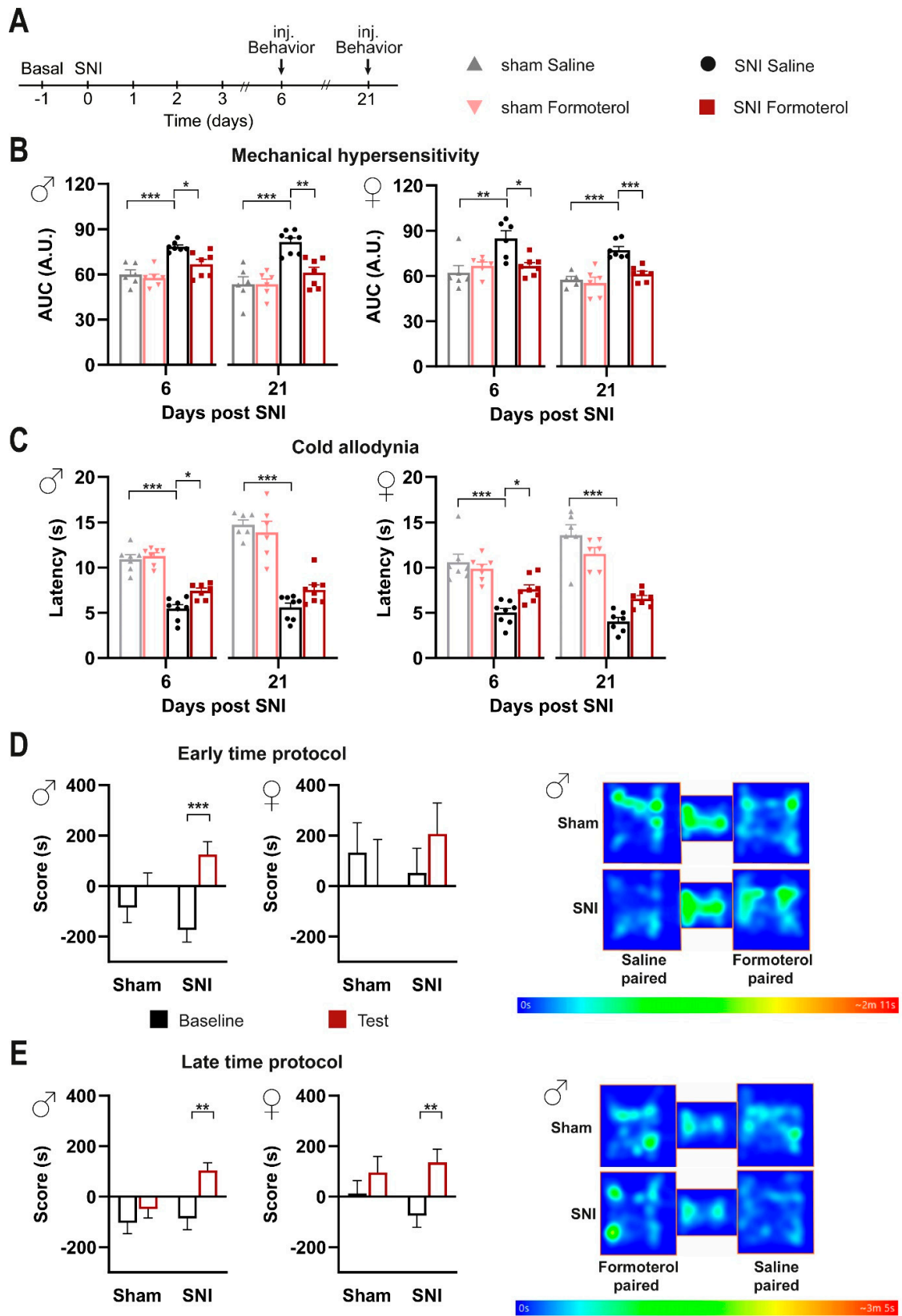


**Figure 2.** Impact of Formoterol on behavior in SNI- and sham-operated WT mice. Conditioned place preference test shows that Formoterol reduces spontaneous pain in SNI-operated mice. (A) Experimental scheme used for testing mechanical sensitivity (von Frey) and cold sensitivity (cold plate) at the plantar hind paw with 8-week-old mice. Inj. = injection. (B) Mechanical sensitivity

was evaluated as integral of the response frequency-von Frey stimulus intensity from 0.008 to 1.0 g (AUC, A.U. = arbitrary unit) six and 21 days after operation in male (left; day 6: F1, 22 = 3.338,  $p = 0.0813$ ; day 21: F1, 23 = 8.048,  $p = 0.0093$ ) and female (right; day 6: F1, 21 = 9.356,  $p = 0.0060$ ; day 21: F1, 21 = 7.224,  $p = 0.0138$ ) mice, injected with saline or Formoterol. (C) Response to cold allodynia six and 21 days post-surgery is indicated as latency (s) of paw withdrawal for males (left; day 6: F1, 25 = 3.972,  $p = 0.0573$ , day 21: F1, 24 = 3.770,  $p = 0.0640$ ) and female (right; day 6: F1, 26 = 7.740,  $p = 0.0099$ ; day 21: F1, 22 = 10.98,  $p = 0.0032$ ) mice.  $n = 6-8$ /group; two-way ANOVA test was performed. \*  $p < 0.05$ , \*\*  $p < 0.01$ , \*\*\*  $p < 0.001$ . Data are expressed as mean  $\pm$  SEM, individual data points are displayed. (D) Conditioned place preference (CPP) was tested to Formoterol at 4 days post-SNI or sham surgery. Analysis of the time spent by operated male (left) or female (right) mice is shown in the Formoterol-paired chamber before (baseline) and after (test) the conditioning. Example of heat maps recorded on the test day. (E) CPP was tested to Formoterol at 32 days post-SNI or sham operation. Score = the time spent by operated male (left) or female (right) mice in the Formoterol-paired chamber on baseline and test day. Representative example of heat maps recorded on the test day.  $n = 6-7$ /sham group;  $n = 8$ /SNI group; two-tailed unpaired  $t$ -test was performed; \*\*  $p < 0.01$ , \*\*\*  $p < 0.001$  as compared between Formoterol-paired chamber baseline and test daytime. Data are indicated as mean  $\pm$  SEM.

In comparison to saline application, Formoterol application at days 6 or 21 post-SNI led to a significant decrease in neuropathic hypersensitivity to mechanical stimuli (Figures 2B and S2A) and cold stimuli (Figure 2C). Indeed, Formoterol injection diminished the exaggerated cumulative response to all the filaments tested (from 0.008 to 1 g) on day 6 and day 21 post-SNI (Figures 2B and S2A). Similar observations were made with respect to allodynia to a cold stimulus on day six post-SNI (Figure 2C). In contrast, Formoterol was not able to significantly inhibit cold allodynia at day 21 post-SNI in both female and male mice (Figure 2C). These data reveal the anti-allodynic effects of systemic Formoterol at late stages after nerve injury and indicate the importance of  $\beta$ 2-AR in mediating these effects at the early and late stages of mechanical allodynia and the early stage of cold allodynia.

Spontaneous pain is a key symptom in patients suffering from neuropathic pain [38]. To study spontaneous pain in mice, we performed a conditioned place preference (CPP) test, in which mice are conditioned to analgesic treatment, such as with pregabalin, in a chamber with specific contextual cues. Preference for the chamber on a day of testing in the absence of pregabalin is employed as a parameter indicative of ongoing pain [39] and the test is well-established in the SNI model [40]. Here, we tested whether Formoterol could induce CPP in a manner similar to pregabalin in neuropathic mice. In the CPP protocol, it is important that analgesia is limited to the time spent in the conditioned chamber, so that the animals can unambiguously associate pain relief with the chamber in which the analgesic drug was administered. Since Formoterol-induced antinociceptive effects last for less than 6 h after a single application, this prerequisite was fulfilled in our experiments (Figure S1C,D). At 8 days post-SNI operation (schematic in Figure S2B), male mice spent more time in the Formoterol-paired chamber post-conditioning, while sham mice did not develop any preference (Figure 2D). In contrast, female SNI mice did not show a statistically significant difference as compared to the sham-operated group, although there was a tendency for increased time spent in the Formoterol-paired chamber (Figures 2D and S2C). To test the relevance of these findings to a more clinically relevant setting of patients with established neuropathic pain, we tested CPP to Formoterol at a late time point, namely 36 days post-SNI (Figures 2E and S2D,E). Compared to the sham mice, male mice with SNI preserved the preference for the Formoterol-paired chamber (Figure 2E). Interestingly, female SNI mice also developed a preference for the Formoterol chamber at this late stage post-SNI (Figures 2E and S2E). These findings suggest that Formoterol can reduce ongoing pain in both male and female mice at late stages post-nerve injury.

### 3.4. *In Vivo Administration of Formoterol Dampens Structural Remodeling and Activation of Microglia in Neuropathic Mice*

Given their role as resident immune cells in the central nervous system (CNS), microglial cells are highly sensitive to inflammatory mediators. In neuropathic pain conditions, several cell types produce a variety of pro-inflammatory substances, many of which can consequentially push microglia toward an inflammatory state [15]. We studied the impact of  $\beta$ 2-AR activation on spinal cord microglia 3, 6 or 21 days after SNI by studying microglial density and morphological changes. The microglia density was analyzed as the density of Iba1-positive cells in the lamina I-III of the SDH (Figure 3A,C). Additionally, microgliosis is differentiated by shifts from ramified-homeostatic microglia towards amoeboid phenotype (enlargement of soma and shortening of processes length). To describe the reactive state of microglia, we studied three hallmarks of microgliosis: density, soma perimeter, and process length (Figure 3). Since it is well known that there are sex differences in microglial contribution to the development and maintenance of neuropathic pain [41], we parsed our analysis based on the sex of mice. We evaluated the ratio between ipsilateral and contralateral SDH, in SNI-operated mice treated with saline or Formoterol. Male mice demonstrated a significant increase in microglial density in the superficial layers of the ipsilateral SDH (marked in dashed lines in examples shown in Figure 3A) at both early and late stages post-SNI (Figure 3C), which was inhibited by Formoterol treatment. In female mice, increased microglial density in the superficial SDH was noted only over early stages post-SNI, which was reversed fully by Formoterol treatment (Figure 3A,B).

In terms of morphological changes in spinal cord microglia in response to nerve injury, we observed that both male and female mice showed a significant increase in the perimeter of microglial cell-body with a corresponding significant decrease in the length of microglia processes over 3, 6 and 21 days post-SNI, although the late stage changes were much more pronounced in male mice as compared to female mice (examples in Figure 3B, quantitative summary in Figure 3D,E and negative controls in Figure S4C). Formoterol partially, but significantly, reversed SNI-induced microglial enlargement of the soma and the shrinking of the processes in male mice at all time points, while it failed to reverse microglial changes at late time points in female mice (Figure 3B,D,E). Interestingly, Formoterol application has no effect on microglia density or morphology in sham-operated mice (Figure S4A,B).

An increase in microglial density does not necessarily correspond to a reactive state of microglia. Hence, to investigate the effect of Formoterol treatment on microglia activation in neuropathic conditions, we performed co-localization analysis using Iba1 as a microglial marker and the active (i.e., phosphorylated) form of two different markers for activation: phosphorylated versions of the MAPKs p38 and JNK. Microglia are the main p38-expressing cells of the spinal cord [42]. JNK signaling modulates apoptosis and the level of pro-inflammatory cytokines, while p38 is involved in the development and maintenance of neuropathic nociceptive hypersensitivity via the induction of inflammatory mediators [3]. Immunoreactivity for phosphorylated p38 in Iba1-expressing microglia was significantly enhanced in male and female mice at early (3 days post-SNI) and late (21 days post-SNI) time points after SNI and was completely reversed by Formoterol treatment at all time points (Figure 4A,B). Phosphorylated JNK was enhanced in microglia of male and female mice at 3, 6 and 21 days post-SNI and was fully reversed by Formoterol in both cases except for female mice at 21 days after SNI operation (Figure 4C,D).

Taken together, analysis of reactive microgliosis after Formoterol treatment in neuropathic mice suggests that Formoterol treatment restores normal microglial morphology and function largely over the development of neuropathic pain in both sexes. Although there was some variability, our analysis suggested that microglial activation is reversed by Formoterol in the late phase after neuropathic pain induction (21 d post-SNI) in male mice, but not in female mice.

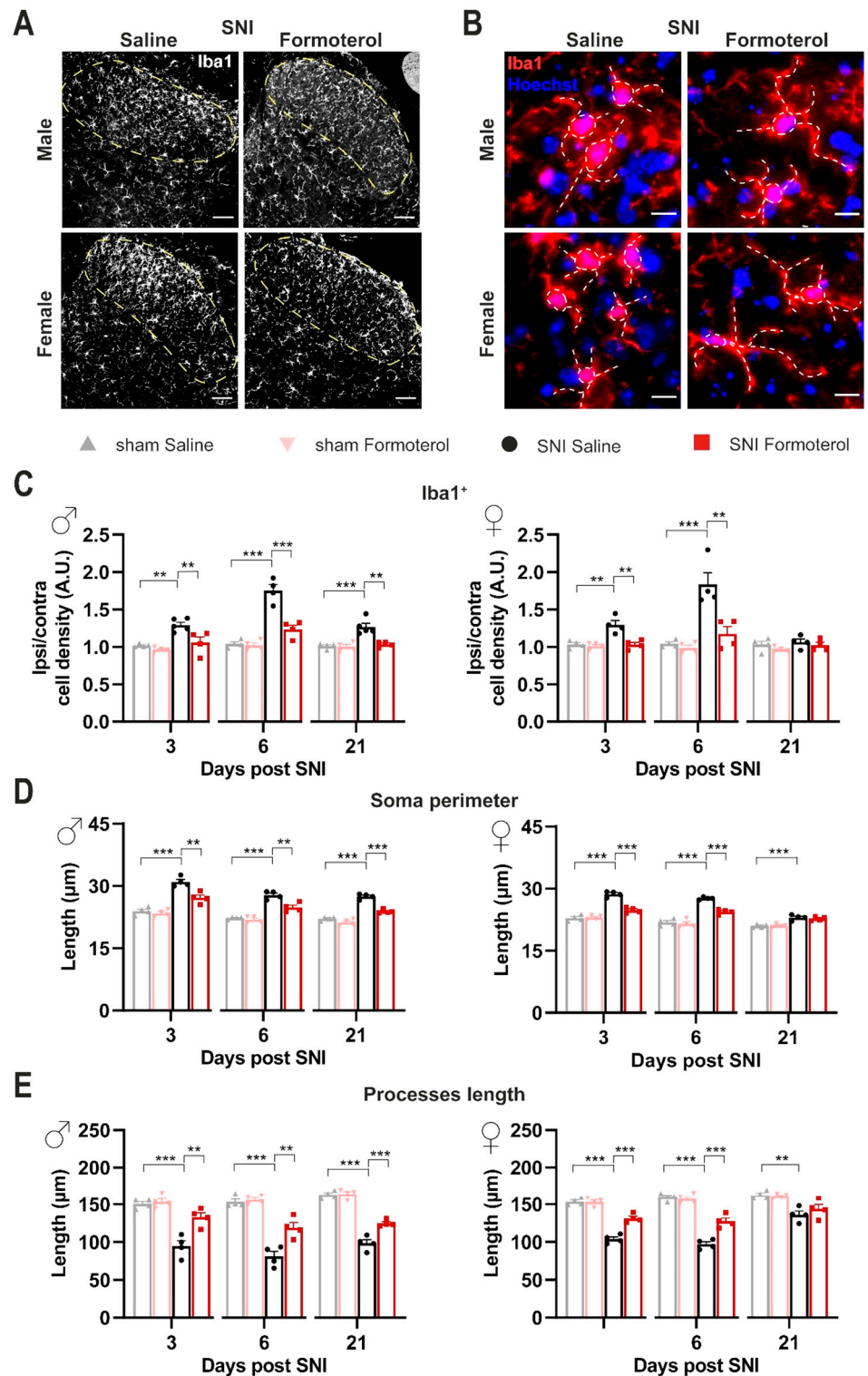


**Figure 3.**  $\beta$ 2-AR agonist diminishes microgliosis in the spinal dorsal horn of SNI-operated mice. (A) Typical examples of Iba1-positive cells in the ipsilateral spinal dorsal horn (SDH) of male or female mice six days after the SNI surgery, injected with saline or Formoterol. Scale bar = 60  $\mu$ m. (B) Representative examples of microglia (Iba1-positive with Hoechst counterstaining for cell nuclei) in the ipsilateral SDH, with somata and processes marked by white, dashed lines, six days after SNI operation injected with saline or Formoterol. Scale bar = 10  $\mu$ m. (C) Analysis of cell density of Iba-1 positive microglia of males (left; day 3: F1, 13 = 4.350,  $p = 0.0573$ ; day 6: F1, 12 = 22.62,  $p = 0.0005$ ; day 21: F1, 13 = 10.86,  $p = 0.0058$ ) and female (right, day 3: F1, 12 = 11.05,  $p = 0.0061$ ; day 6: F1, 12 = 10.28,

$p = 0.0075$ ; day 21:  $F_{1, 12} = 0.09192$ ,  $p = 0.7669$ ) treated with Formoterol or saline 3, 6 and 21 days after the operation. Ipsi/contra = ratio between the density value of the ipsilateral and contralateral SDH. A.U. = arbitrary unit. (D,E) Analysis of microglia morphology; the perimeter of the soma (D) and the processes length (E) in Formoterol- or saline-injected male (left; soma day 3:  $F_{1, 12} = 9.207$ ,  $p = 0.0104$ ; soma day 6:  $F_{1, 12} = 9.737$ ,  $p = 0.0088$ ; soma day 21:  $F_{1, 12} = 22.64$ ,  $p = 0.0005$ ; processes day 3:  $F_{1, 12} = 10.89$ ,  $p = 0.0063$ ; processes day 6:  $F_{1, 12} = 10.78$ ,  $p = 0.0065$ ; processes day 21:  $F_{1, 12} = 14.27$ ,  $p = 0.0026$ ) and female (right, soma day 3:  $F_{1, 12} = 37.65$ ,  $p < 0.0001$ ; soma day 6:  $F_{1, 12} = 16.83$ ,  $p = 0.0015$ ; soma day 21:  $F_{1, 12} = 0.4001$ ,  $p = 0.5389$ ; processes day 3:  $F_{1, 12} = 26.86$ ,  $p = 0.0002$ ; processes day 6:  $F_{1, 12} = 20.92$ ,  $p = 0.0006$ ; processes day 21:  $F_{1, 12} = 1.159$ ,  $p = 0.3028$ ) mice 3, 6, or 21 days after surgery.  $n = 4-5$ /group; two-way ANOVA test was performed; \*\*  $p < 0.01$ , \*\*\*  $p < 0.001$ . Data are shown as mean  $\pm$  SEM, individual data points are displayed.

### 3.5. Formoterol Diminishes Astrocytic Activation at Late Stages after Nerve Injury in Female Mice

Astrocytes also express  $\beta_2$ -AR; therefore, Formoterol might exert its analgesic effect through the activation of this receptor on astrocytes. Using the same experimental protocol, we studied the effect of  $\beta_2$ -AR activation on astrocytes using Glial fibrillary acidic protein (GFAP) to identify astrocytes in combination with a classic activation marker, p-JNK. In both sexes, we observed a significant increase in GFAP signal intensity at late time points after nerve injury (21 d post-SNI) when neuropathic pain is fully developed, but not over early time points (Figure 5A,B). Interestingly, SNI-induced astrogliosis was partially, but significantly, inhibited by Formoterol in both sexes (Figure 5A,B).

These findings are in line with the emerging view that microglia are activated during an acute phase and drive neuroinflammation, which leads to the transition of acute pain into chronic pain, while spinal cord astrocytes contribute to central sensitization and the maintenance of chronic pain [41]. Interestingly, nerve injury also induced upregulation of p-JNK in GFAP-positive astrocytes in female mice at 6 and 21 days post-SNI, which was reversed by Formoterol (Figure 5C,D). Neither p-JNK upregulation in astrocytes nor effects of Formoterol were reliably seen in male and female mice at early time points post-SNI (Figure 5D).

These results suggest a disconnection between the role of  $\beta_2$ -ARs in early microglial changes and late astrogliosis. However, there is ample literature suggesting that early microglial activation is linked to late astrocytic involvement in neuropathic pain. In our analyses, because Formoterol was sequentially administered at 6 and 21 days, it could not be ruled out that the Formoterol effects seen at 21 days (mostly involving astrocytes) were aided by the injection of Formoterol at 6 days post-SNI that reduces the microglial pro-inflammatory response. To dissect these from one another, we performed an additional experiment in which Formoterol was only injected at 21 days post-SNI in wild-type mice (scheme shown in Figure S3A). Interestingly, in both sexes, the single late injection of Formoterol significantly reduced mechanical hypersensitivity (Figure S3B), and the magnitude of this change was comparable to that of our previous experiment in which Formoterol had been injected at 6 and 21 days post-SNI. Similar results were obtained for the cold allodynia test (Figure S3C). Microglial density in the SDH was not significantly changed by the single late application of Formoterol in mice of both sexes (Figure S3D,E). Finally, astrogliosis seen at the late time point post-SNI was significantly reduced by Formoterol given as a single application on day 21 post-SNI (Figure S3F,G). Taken together, these results demonstrate that Formoterol effects at late time points are not dependent on the application of Formoterol at early stages after nerve injury and suggest a disconnection between  $\beta_2$ -AR modulation in microglia and astrocytes.

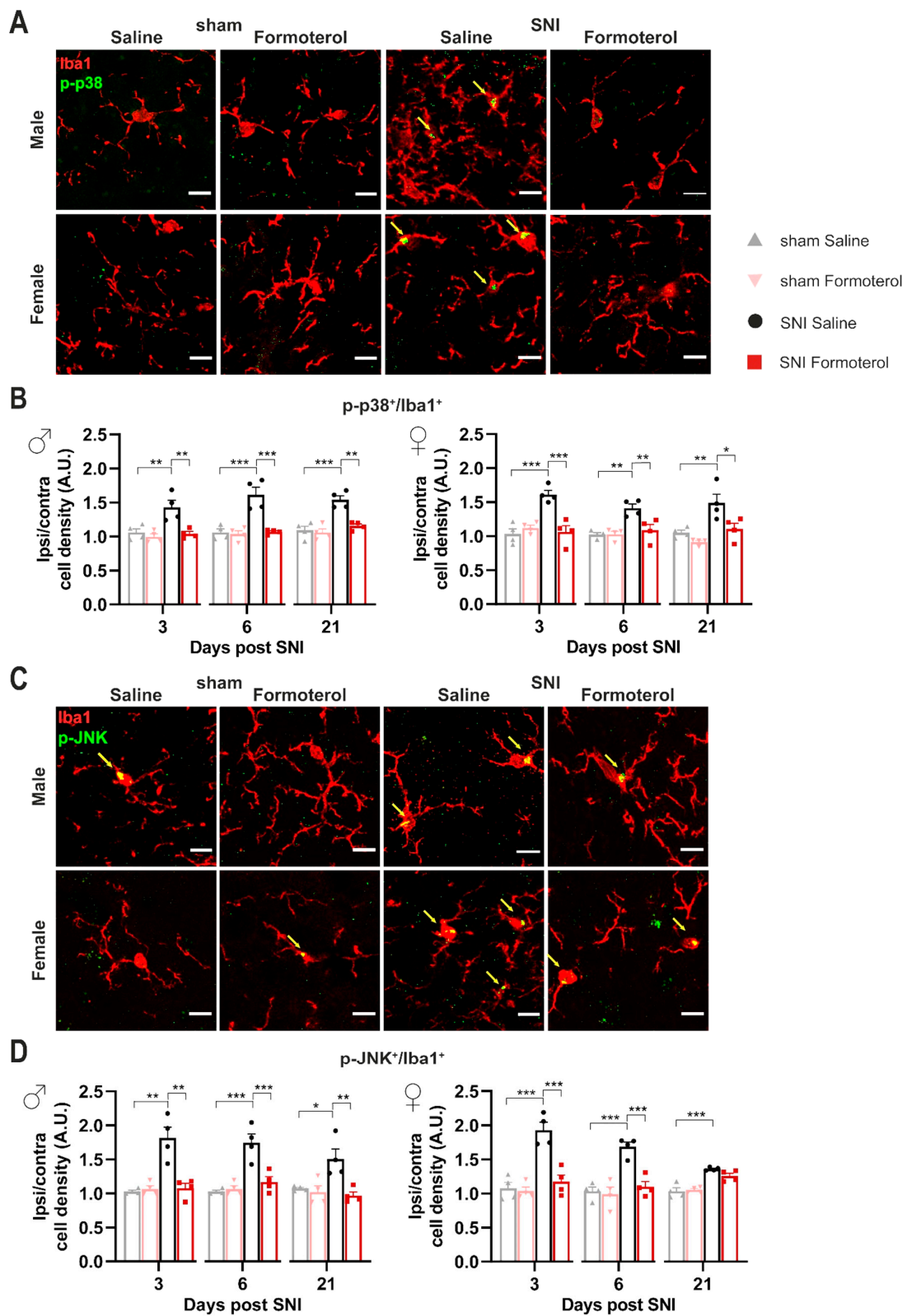


**Figure 4.** Formoterol weakens microglial activation markers in the spinal dorsal horn of SNI-operated mice. (A) Representative examples of colocalization of Iba1-positive signal and the microglial activation marker p-p38 in the ipsilateral spinal dorsal horn (SDH) in male and female mice, six days after operation injected with saline or Formoterol. Double-positive cells are pointed by arrows.

Scale bar = 10  $\mu$ m. (B) Colocalization analysis of the activity marker p-p38 and Iba1 immunohistochemistry 3, 6 and 21 days after surgery in male (left; day 3: F1, 12 = 6.529,  $p = 0.0252$ ; day 6: F1, 12 = 15.50,  $p = 0.0020$ ; day 21: F1, 12 = 11.09,  $p = 0.0060$ ) and female (right; day 3: F1, 12 = 12.52,  $p = 0.0041$ ; day 6: F1, 12 = 8.325,  $p = 0.0137$ ; day 21: F1, 12 = 11.01,  $p = 0.0061$ ) mice. (C) Images of Iba1 and p-JNK positive signals in the ipsilateral SDH of male and female mice, six days post-surgery, injected with saline or Formoterol. Double-positive cells are pointed by arrows. Scale bar = 10  $\mu$ m. (D) Analysis of the colocalization of Iba1-positive signal and the activation marker p-JNK in the spinal dorsal horn of male (left; day 3: F1, 12 = 9.548,  $p = 0.0094$ ; day 6: F1, 12 = 15.84,  $p = 0.0018$ ; day 21: F1, 12 = 7.225,  $p = 0.0197$ ) and female (right; day 3: F1, 12 = 15.09,  $p = 0.0022$ ; day 6: F1, 12 = 12.27,  $p = 0.0044$ ; day 21: F1, 12 = 3.269,  $p = 0.0957$ ) mice treated with saline or Formoterol, three, six, and 21 days after the operation. Ipsi/contra = ratio between the ipsilateral and contralateral dorsal horn of the spinal cord. A.U. = arbitrary unit.  $n = 4$ /group; two-way ANOVA test was performed; \*  $p < 0.05$ , \*\*  $p < 0.01$ , \*\*\*  $p < 0.001$ . Data are shown as mean  $\pm$  SEM, individual data points are displayed.

### 3.6. Contribution of Microglial $\beta$ 2-ARs to Anti-Nociceptive Effects of Formoterol in Mice with Neuropathic Pain

Our analyses uncovered the potential of systemically applied Formoterol in inhibiting microglia activation in neuropathic pain conditions. Therefore, we addressed the contributions of microglial  $\beta$ 2-AR to Formoterol-induced analgesia, given their broad expression across cell types. To test the importance of the microglial  $\beta$ 2-AR, we generated a conditional knockout mouse line in which the *Adrb2* gene was specifically deleted from microglia cells (strategy shown schematically in Figure 6A). We crossbred *Cx3cr1-CreERT2* mice with the *Adrb2* floxed mice to generate double transgenic mice *Cx3cr1-CreERT2; Adrb2<sup>fl/fl</sup>* mice. *Cx3cr1-Adrb2<sup>fl/fl</sup>* and control (*Adrb2<sup>fl/fl</sup>*) mice were injected with tamoxifen at 5 weeks of age, and post 3–4 weeks qPCR analysis on MAC sorted microglial cells showed more than an 80% reduction in the expression of *Adrb2* in *Cx3cr1-Adrb2<sup>fl/fl</sup>* mice when compared to control mice or *Cx3cr1-Adrb2<sup>fl/fl</sup>* mice not injected with tamoxifen (Figure 6B).

Importantly, the deletion of  $\beta$ 2-ARs specifically in microglia does not significantly affect the course of allodynia/hyperalgesia following SNI. Indeed, *Cx3cr1-Adrb2<sup>-/-</sup>* mice show similar baseline sensitivity and development of hypersensitivity following SNI operation comparable with those of control mice (Figure 6C,D, time points Basal and 3 days after SNI). In comparison to saline application, Formoterol application at days 6 or 21 post-SNI led to a significant decrease in neuropathic hypersensitivity to mechanical stimuli (Figure 6D,E) and cold stimuli (Figure 6F) in control mice, but not in *Cx3cr1-Adrb2<sup>-/-</sup>* mice (Figure 6D,F). Figure 6D shows the response frequency to a von Frey stimulation at 0.07 g force, which at basal condition elicits almost no responses, but leads to exaggerated response frequency at 6 and 21 days post-SNI. However, after 1 h i.p. injection of Formoterol, the mechanical hypersensitivity is fully reversed to baseline levels in control mice but not in *Cx3cr1-Adrb2<sup>-/-</sup>* mice, thereby, suggesting that microglial  $\beta$ 2-AR is required for Formoterol-induced analgesia. In *Cx3cr1-Adrb2<sup>-/-</sup>* mice, Formoterol failed to attenuate the exaggerated cumulative response to all the von Frey filaments tested on control mice, on day 6 and day 21 post-SNI (Figure 6E). Mice of both sexes showed a comparable loss of Formoterol-induced analgesia and there was no apparent sexual dimorphism. Similar observations were made with respect to allodynia to a cold stimulus on day 6 and day 21 post-SNI. Indeed, the analgesic effect of Formoterol related to cold stimuli was lost in *Cx3cr1-Adrb2<sup>-/-</sup>* mice (Figure 6F). These data reveal the anti-allodynic effects of systemic Formoterol at late stages after nerve injury and indicate the crucial role of microglial  $\beta$ 2-AR in mediating the analgesic effects at early and late stages of mechanical allodynia and cold allodynia.



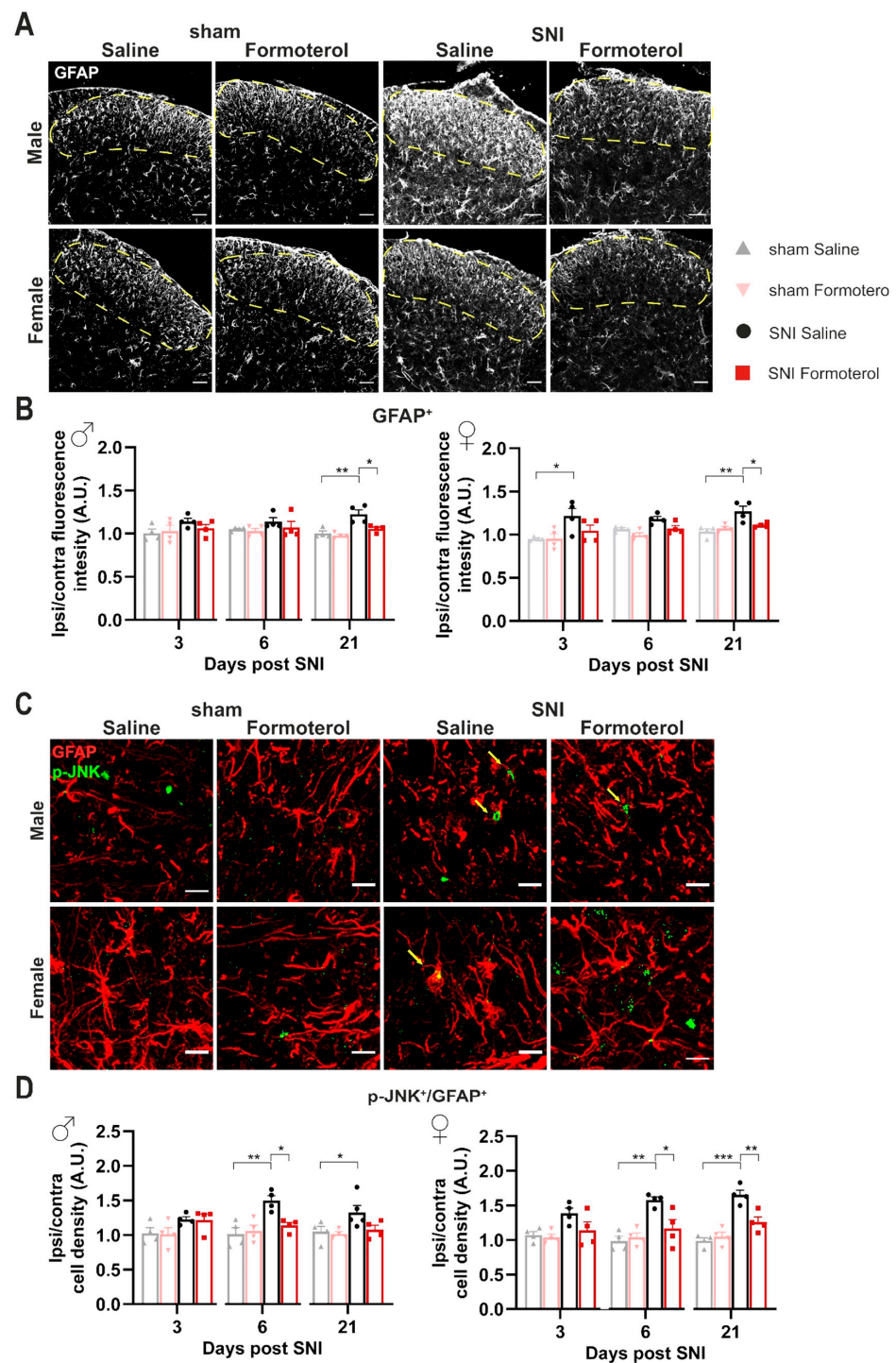


**Figure 5. Spinal astroglial cells response to Formoterol in SNI-operated wild-type mice.** (A) Examples of GFAP immune reactivity in the ipsilateral spinal dorsal horn (SDH) 21 days after nerve injury in male and female WT mice who received saline or Formoterol injection. Scale bar = 60  $\mu$ m. (B) Analysis of GFAP fluorescent intensity of male (left; day 3: F1, 12 = 1.097,  $p = 0.3156$ ; day 6: F1, 12 = 0.9393,  $p = 0.3516$ ; day 21: F1, 12 = 5.003,  $p = 0.0451$ ) and female (right; day 3: F1, 12 = 1.835,  $p = 0.2005$ ; day 6: F1, 12 = 0.4848,  $p = 0.4995$ ; day 21: F1, 12 = 8.059,  $p = 0.0149$ ) WT mice treated with saline or Formoterol, 3, 6 and 21 days after the operation. Ipsi/contra fluorescent intensity = ratio between values of fluorescent intensity obtained from the ipsilateral and contralateral

SDH. (C) Typical examples of colocalization of GFAP astrocytic marker with glial activation marker, p-JNK in the ipsilateral SDH of male and female mice, 21 days after sham or SNI operation in mice injected with saline or Formoterol. Scale bar = 10  $\mu$ m. (D) Quantitative analysis of the colocalization of GFAP and the activation marker p-JNK in the SDH of male (left; day 3: F1, 12 = 0.02015,  $p$  = 0.8895; day 6: F1, 12 = 7.089,  $p$  = 0.0207; day 21: F1, 13 = 2.850,  $p$  = 0.1152) and female (right; day 3: F1, 12 = 1.759,  $p$  = 0.2095; day 6: F1, 12 = 8.117,  $p$  = 0.0146; day 21: F1, 12 = 12.89,  $p$  = 0.0037) mice treated with saline, or Formoterol, 3, 6 and 21 days after sham or SNI operation. Ipsi/contra = ratio between the ipsilateral and contralateral SDH. A.U. = arbitrary unit.  $n$  = 4/group; two-way ANOVA test. \*  $p$  < 0.05, \*\*  $p$  < 0.01, \*\*\*  $p$  < 0.001. Data are indicated as mean  $\pm$  SEM, individual data points are displayed.

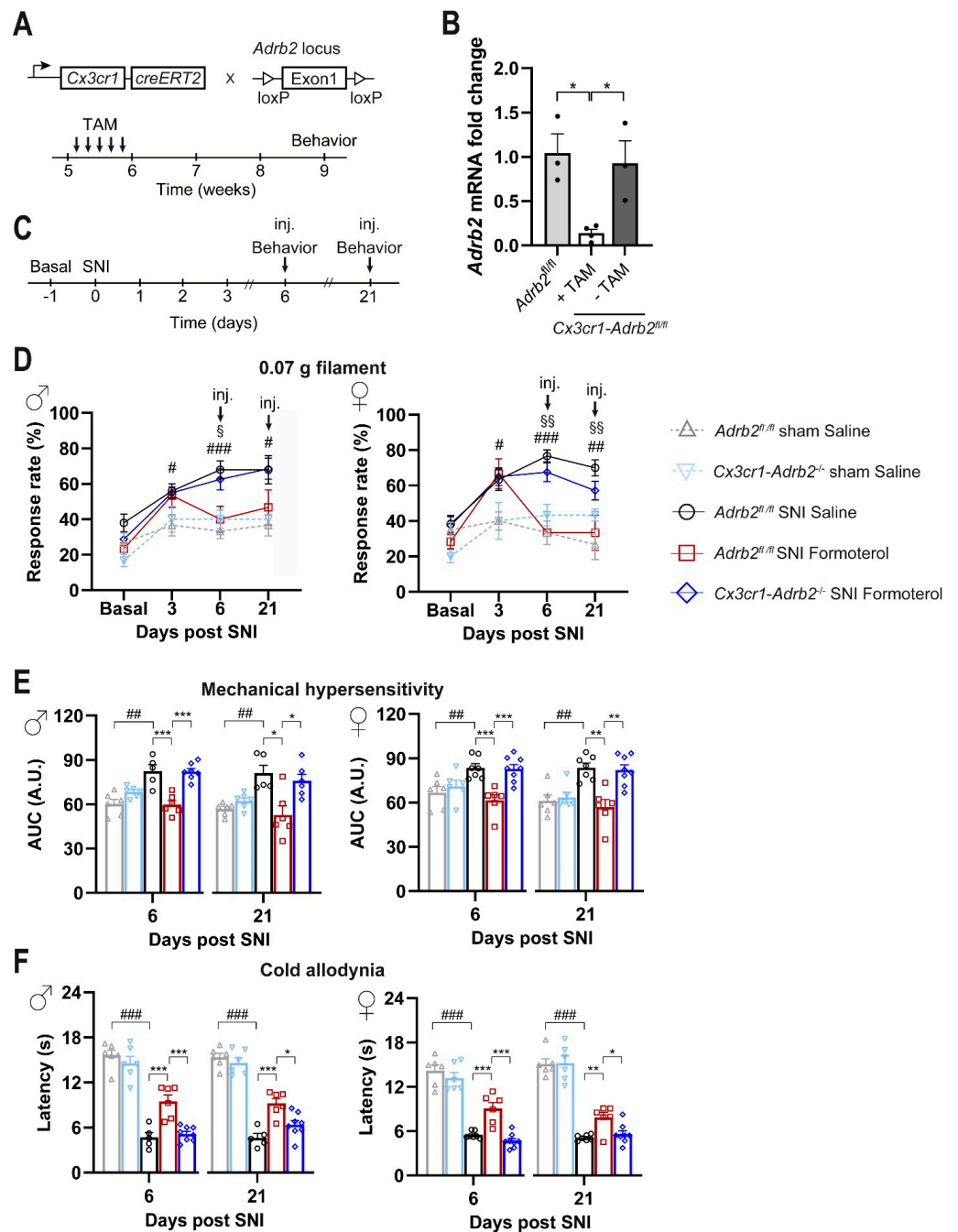


Figure 6. Effect of Formoterol on behavior in *Cx3cr1-Adrb2<sup>-/-</sup>* operated mice. (A) Schematic representation of the strategy for generation of mice lacking the *Adrb2* gene conditionally in microglial cells in a tamoxifen-inducible manner. (B) Analysis via qPCR demonstrating the loss of *Adrb2* mRNA

expression in microglia cells three weeks after tamoxifen injection in the mouse line *Cx3cr1-Adrb2<sup>fl/fl</sup>*. The recombination does not occur in mice lacking the Cre-cassette (*Adrb2<sup>fl/fl</sup>*). TAM = Tamoxifen. n = 3–4/group; ordinary two-way ANOVA with main effects only was performed. \*  $p < 0.05$ . (C) Experimental scheme for testing mechanical sensitivity (von Frey) and cold allodynia (cold plate) at the plantar hind paw with 8–9 weeks old mice. Inj. = injection. (D) Mechanical sensitivity is displayed as response frequency to the 0.07 g filament in male (left) and female (right) control mice (grey line for *Adrb2<sup>fl/fl</sup>* sham saline-injected mice; pink line for *Cx3cr1-Adrb2<sup>-/-</sup>* sham saline-injected mice black line for *Adrb2<sup>fl/fl</sup>* SNI saline-injected mice; red line for *Adrb2<sup>fl/fl</sup>* SNI Formoterol-injected mice) and *Cx3cr1-Adrb2<sup>-/-</sup>* transgenic mice (blue line) before the SNI operation (basal measurement), 3 days after surgery, and 6 and 21 days after the SNI, 1 hour after Formoterol injection. n = 5–8/group; *t*-test test was performed; §  $p < 0.05$ , §§  $p < 0.01$  as compared *Cx3cr1-Adrb2<sup>-/-</sup>* SNI Formoterol and *Adrb2<sup>fl/fl</sup>* SNI Formoterol; #  $p < 0.05$ , ##  $p < 0.01$ , ###  $p < 0.001$  as compared *Adrb2<sup>fl/fl</sup>* SNI Saline and *Adrb2<sup>fl/fl</sup>* Sham Saline. (E) Mechanical sensitivity of the same groups as (D) shown as integral of the response frequency-von Frey stimulus intensity from 0.008 to 1.0 g (AUC, A.U. = arbitrary unit). (F) Cold sensitivity 6 and 21 days after SNI or sham surgery, after Formoterol or saline injection showed as latency (s) of paw withdrawal. n = 5–8/group; *t*-test test was performed; ##  $p < 0.01$ , ###  $p < 0.001$  as compared *Adrb2<sup>fl/fl</sup>* sham saline and *Adrb2<sup>fl/fl</sup>* SNI saline; ordinary two-way ANOVA with main effects only was performed among *Adrb2<sup>fl/fl</sup>* SNI saline, *Adrb2<sup>fl/fl</sup>* SNI Formoterol, and *Cx3cr1-Adrb2<sup>-/-</sup>* SNI Formoterol; \*  $p < 0.05$ , \*\*  $p < 0.01$ , \*\*\*  $p < 0.001$ . Data are expressed as mean  $\pm$  SEM, individual data points are exhibited.

### 3.7. Contribution of Microglial $\beta$ 2-ARs to Inhibitory Effects of Formoterol on SNI-Induced Microgliosis and Astrogliosis

Furthermore, we analyzed if deleting the microglial  $\beta$ 2-AR influenced the accumulation of microglia in the SDH and the increased GFAP expression in activated astrocytes that are typical for SNI after 6 and 21 days post-nerve injury. Indeed, in contrast to control mice, Formoterol treatment failed to decrease the density of microglia in the ipsilateral SDH of *Cx3cr1-Adrb2<sup>-/-</sup>* mice of both sexes 6 and 21 days after SNI operation (Figure 7A,B), further supporting a role of  $\beta$ 2-AR activation in the modulation of microglial reactivity and in the induction of neuropathic pain.

In addition, Formoterol application failed to revert SNI-dependent morphological changes in *Cx3cr1-Adrb2<sup>-/-</sup>* mice (Figure 7C,D), underlining the crucial role of microglial  $\beta$ 2-AR for the analgesic effect of Formoterol. To confirm the role of microglial  $\beta$ 2-AR in mediating the effect of Formoterol, we checked the expression of microglial activity markers (p-p38 and p-JNK) in mice that lost  $\beta$ 2-AR receptors. As expected, contrary to what happened in control mice, in both male and female *Cx3cr1-Adrb2<sup>-/-</sup>* mice Formoterol failed to damp the upregulation of microglial activity marker typically seen 6 and 21 days after SNI (Figure 8).

As with control mice, in *Cx3cr1-Adrb2<sup>-/-</sup>* of both sexes, we observed a significant increase in GFAP signal intensity at late time points (three weeks post-SNI) when neuropathic pain is fully established, but not over early time points, which was partially, but significantly, inhibited by Formoterol (Figure 9A,B). Interestingly, the nerve injury-induced upregulation of p-JNK in GFAP-positive cells in *Cx3cr1-Adrb2<sup>-/-</sup>* female mice at 6 and 21 days post-SNI was reversed by Formoterol (Figure 9C,D). Neither p-JNK upregulation nor effects of Formoterol were reliably seen in male and female mice at early time points after SNI (Figure 9D). This data indicates that at late time points after SNI operation, the contribution of the microglial  $\beta$ 2-ARs to the effect of Formoterol is minimal.

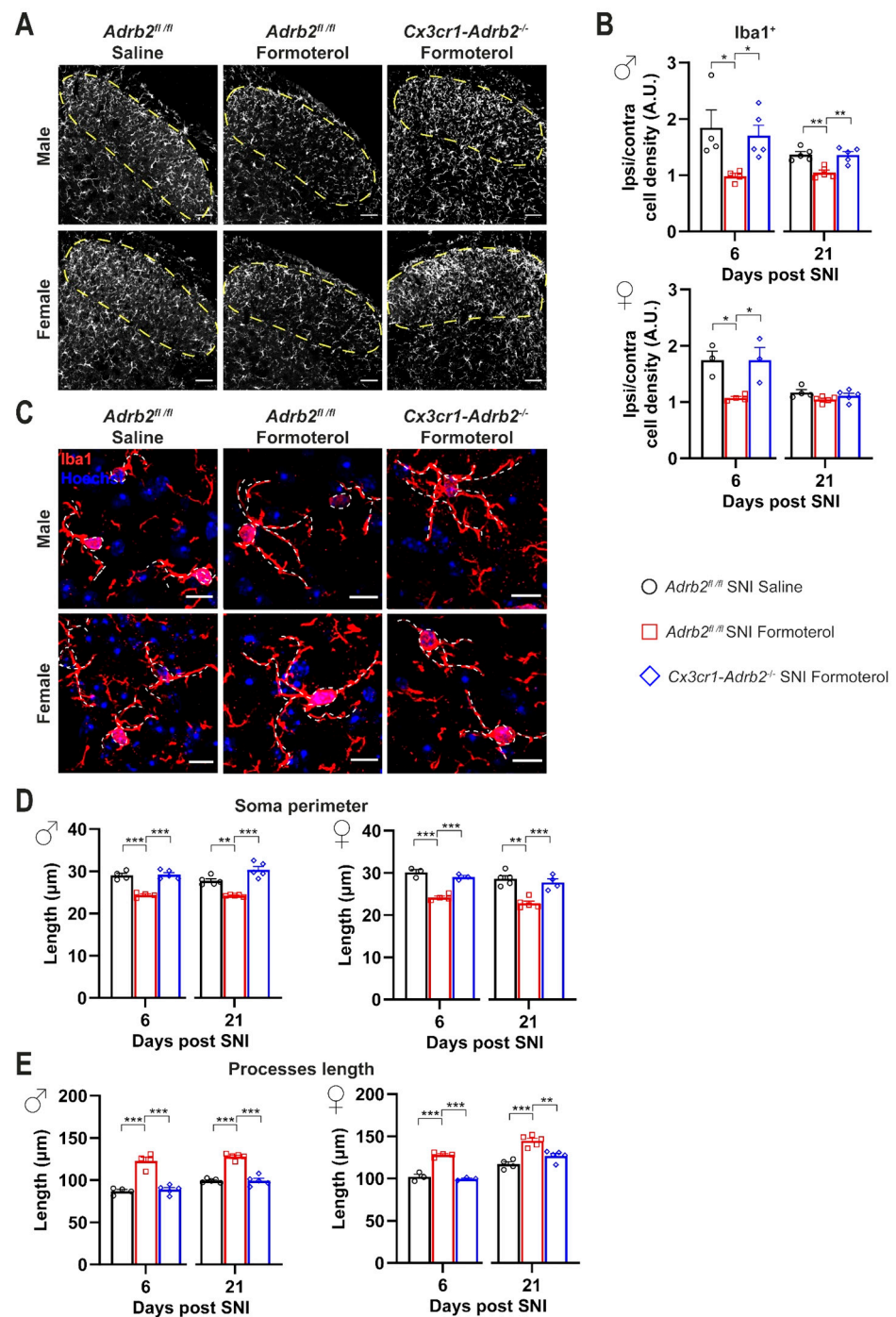


**Figure 7. Spinal microglia response to the  $\beta$ 2-AR agonist in SNI-operated control and transgenic mice.** (A) Typical examples of Iba1-positive staining in the ipsilateral spinal dorsal horn (SDH) six days post nerve injury in control and transgenic mice who received saline or Formoterol injection. Scale bar = 60  $\mu$ m. (B) Quantitative analysis of microglia density (Iba1-positive cells) of control and *Cx3cr1-Adrb2<sup>-/-</sup>* male (left) and female (right) mice treated with saline, or Formoterol, 6 and 21 days after SNI operation. Ipsi/contra = ratio between the ipsilateral and contralateral SDH. A.U. = arbitrary unit. (C) Representative examples of microglia in the ipsilateral SDH in male and female mice, with somata and processes marked by white, dashed lines, six days after SNI operation injected with saline or Formoterol. Scale bar = 10  $\mu$ m. (D,E) Formoterol and saline application to control and transgenic male (left) and female (right) mice 6 or 21 days after SNI influences microglial morphological parameters: the perimeter of the soma (D) and the processes length (E). n = 3–5/group; ordinary two-way ANOVA with main effects only was performed; \*  $p < 0.05$ , \*\*  $p < 0.01$ , \*\*\*  $p < 0.001$ . Data are shown as mean  $\pm$  SEM, individual data points are indicated.

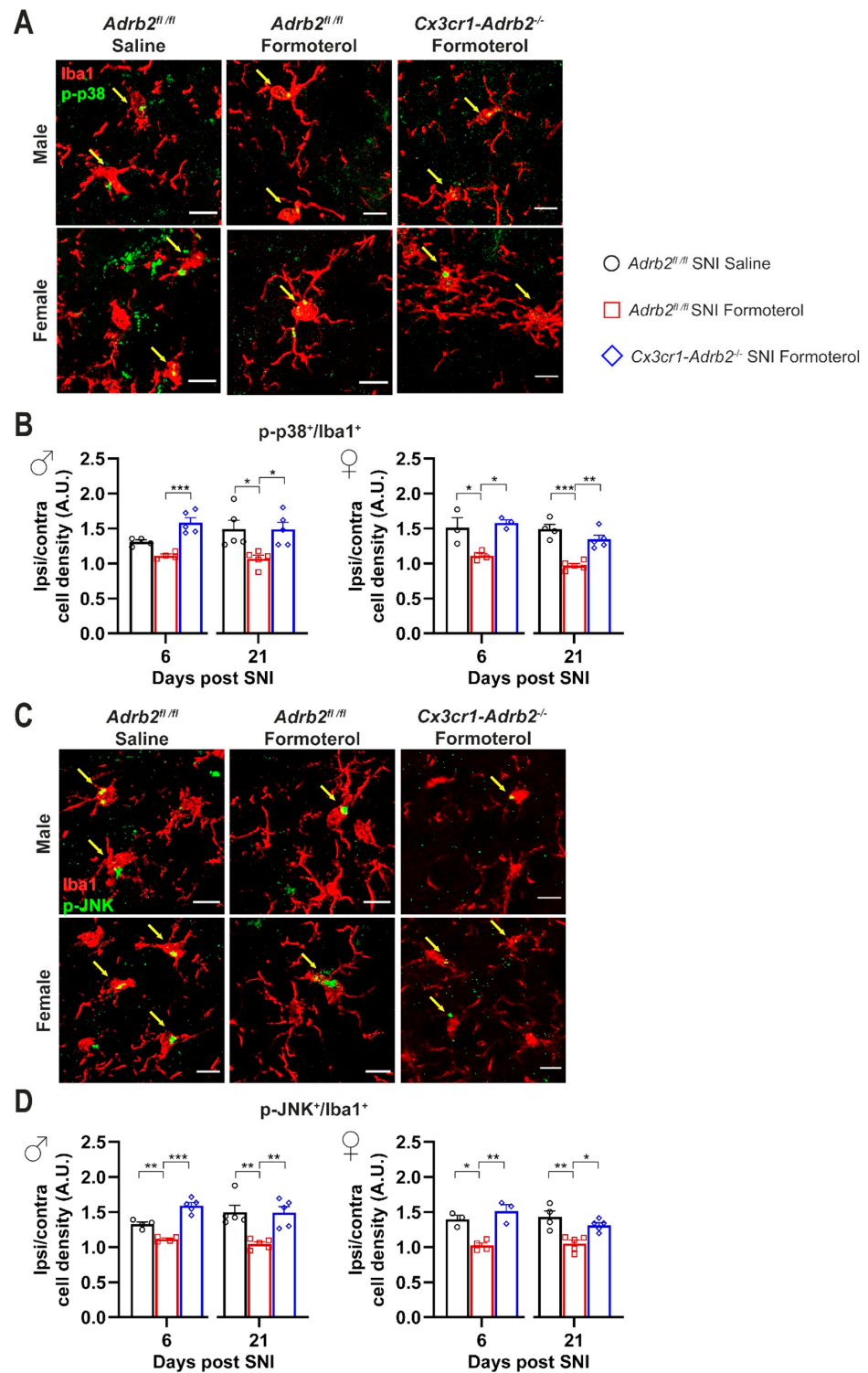


**Figure 8.** Microglial  $\beta$ 2-AR knockdown impairs the Formoterol effect of lowering microglial activation markers levels in the ipsilateral spinal dorsal horn of SNI-operated mice. (A) Typical examples of colocalization of Iba1-positive cells and p-p38, the microglial activation markers in the spinal dorsal horn (SDH) of male and female mice, six days after SNI operation in control and transgenic mice injected with saline or Formoterol. Double-positive cells are pointed by arrows. Scale bar = 10  $\mu$ m. (B) Analysis of the co-staining of Iba-1 immunohistochemistry and p-p38 of control and *Cx3cr1-Adrb2*<sup>-/-</sup> male (left) and female (right) mice treated with saline or Formoterol, 6 and 21 days after SNI operation. Ipsi/contra = ratio between the ipsilateral and contralateral dorsal

horn of the spinal cord. A.U. = arbitrary unit. (C) Representative images of Iba1-positive signal and p-JNK in the SDH six days after surgery, one hour from saline or Formoterol injection. Double-positive cells are pointed by arrows. Scale bar = 10  $\mu$ m. (D) Quantification of Iba1 and p-JNK co-staining of control and *Cx3cr1-Adrb2*<sup>-/-</sup> male (left) and female (right) mice treated with saline or Formoterol, 6 and 21 days after surgery. n = 3–5/group; ordinary two-way ANOVA with main effects only was performed; \* *p* < 0.05, \*\* *p* < 0.01, \*\*\* *p* < 0.001. Data are shown as mean  $\pm$  SEM, individual values are also displayed.

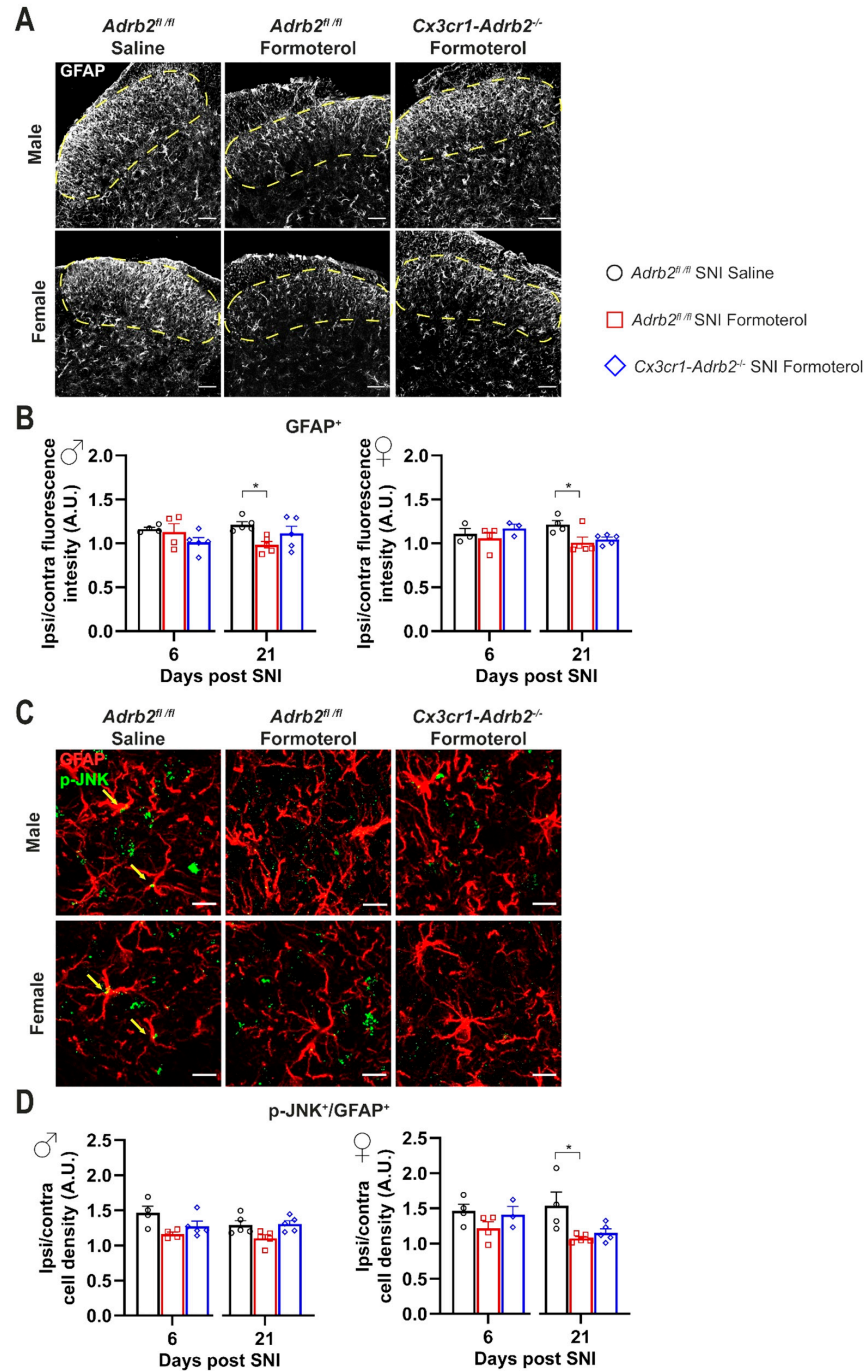


**Figure 9.** The knockdown of the microglial  $\beta$ 2-AR did not affect the astrocytic response to Formoterol. (A) Examples of GFAP immune reactivity in the ipsilateral spinal dorsal horn 21 days after nerve injury in control and transgenic mice who received saline or Formoterol injection. Scale bar = 60  $\mu$ m. (B) Analysis of GFAP fluorescent intensity of control and *Cx3cr1-Adrb2*<sup>-/-</sup> mice treated

with saline, or Formoterol, 6 and 21 days after SNI operation. Ipsi/contra fluorescent intensity = ratio between values of fluorescent intensity obtained from the ipsilateral and contralateral SDH. (C) Representative examples of colocalization of GFAP astrocytic marker with glial activation marker, p-JNK in the ipsilateral SDH of male and female mice, 21 days after SNI operation in mice injected with saline or Formoterol. Scale bar = 10  $\mu\text{m}$ . (D) Quantitative analysis of the colocalization of GFAP and the activation marker p-JNK in the SDH of male (left) and female (right) mice treated with saline, or Formoterol, 6 and 21 days after SNI operation. Ipsi/contra = ratio between the ipsilateral and contralateral SDH. A.U. = arbitrary unit.  $n = 3\text{--}5/\text{group}$ ; ordinary two-way ANOVA with main effects only was performed. \*  $p < 0.05$ . Data are shown as mean  $\pm$  SEM, individual data points are given.

#### 4. Discussion

New therapies and deeper mechanistic insights are urgently needed for the clinical management of neuropathic pain. Noradrenergic signaling has long been known to play a key role in the pathophysiological sequelae leading to chronic pain, and drugs activating inhibitory ( $\alpha 2$ ) noradrenergic receptors, such as clonidine, have been subject to intense clinical and preclinical investigation in the past [1,43]. The present study now sets a focus on investigating glial noradrenergic signaling and its contributions via a mechanistically distinct class of receptors, namely excitatory receptors of the  $\beta 2$ -type.

A few studies have reported beneficial effects of  $\beta 2$ -AR agonists, such as terbutaline, on diverse types of inflammatory pain and, more recently, pain of neuropathic origin [44,45]. In these studies, the authors show that, in the context of neuropathic pain, peripheral  $\delta$  opioid (DOP) receptors expressed in Nav1.8+ neurons are required for the analgesic effect of  $\beta 2$ -AR agonist Formoterol. However, the mechanistic link between these two receptor systems, opioids and adrenergic, is yet to be explored as well as the precise mode of action and the stage at which  $\beta 2$ -AR activation would exhibit the best therapeutic effects on neuropathic pain remains unclear.

Here, we studied the impact of the pharmacological activation of  $\beta 2$ -ARs on glial cells on the distinct phases of development and maintenance of neuropathic pain in the SNI model of neuropathic pain. This study goes beyond confirming previous positive reports on  $\beta 2$ -ARs and reveals several novel insights, including: (i)  $\beta 2$ -ARs expressed by microglia are required for the anti-allodynic effects of  $\beta 2$ -AR agonists; (ii)  $\beta 2$ -AR activation modulates different aspects and modalities of neuropathic pain in a stage-specific manner; (iii)  $\beta 2$ -AR-mediated anti-allodynic actions at different temporal phases of neuropathic pain differentially involve microglia and astrocytes; and (iv)  $\beta 2$ -AR activation not only suppresses the sensory component of neuropathic pain but also reduces negative affect at a time when neuropathic pain is chronically established.

Several observations support the view that  $\beta 2$ -AR agonists exert analgesic actions in neuropathic pain primarily via microglia, at least over the period from early establishment of neuropathic hypersensitivity. First, we found that Formoterol induces strong molecular alterations in pure populations of microglia that promote an anti-inflammatory phenotype. Secondly, nerve injury-induced alterations in native populations of microglia in spinal dorsal horn circuits were fully reversed by Formoterol. Formoterol-induced suppression of microgliosis did not occur in mice with a microglia-specific loss of  $\beta 2$ -ARs, showing that modulation of microglial function by Formoterol occurs via direct actions on  $\beta 2$ -ARs in microglia and not downstream of  $\beta 2$ -AR actions in other cell types that engage in paracrine signaling with microglia. Remarkably, Formoterol-induced reversal of neuropathic pain-associated behaviors was fully abrogated in mice with a microglia-specific loss of  $\beta 2$ -ARs in both male and female mice. These findings suggest that over the initial phase post-injury when neuropathic pain develops, pro-inflammatory spinal cord microglial signaling can be hindered by the therapeutic use of  $\beta 2$ -AR agonists to put brakes on the sequence of pathophysiological events that lead to the full manifestation of neuropathic pain.

$\beta 2$ -ARs are expressed on the astrocytes, and indeed we observed inhibition of astrocyte activation by Formoterol in nerve-injured mice at later stages when neuropathic pain was chronically established in female mice. However, there is evidence of sequential activation of microglia early post-injury and astrocytes thereafter, and there are strong indications

of crosstalk between microglia and astrocytes. Our data indicate that  $\beta$ 2-AR signaling is not involved in this crosstalk and that noradrenergic signaling in microglia and astrocytes occurs independently of each other. Our finding that Formoterol is efficacious in reducing allodynia when given at a late stage alone, and that this late effect is not mediated by microglial  $\beta$ 2-AR, implies that there are at least two temporally distinct modes of action for the anti-allodynic effects of Formoterol: an early effect via microglia and a late effect via astrocytes. This implies that when patients seek therapy at late stages post-nerve injury when neuropathic pain has already become chronic, Formoterol can still be efficacious by acting via  $\beta$ 2-AR in astrocytes. It must be acknowledged, however, that this study was limited to microglial manipulations and further studies involving the astrocyte-specific deletion of *Adbl2* will further elucidate the role of astrocytes on the development and maintenance of chronic pain.

This provides a new way of action on the current therapeutic applications of SNRIs, such as Duloxetine in neuropathic pain. SNRIs act by increasing NA availability for signaling in neural pathways and our results suggest that SNRIs-induced analgesia is likely to involve  $\beta$ 2-AR signaling in microglia [46,47]. Our observation that  $\beta$ 2-AR expression increases in microglia after nerve injury is supportive of this hypothesis. Furthermore, since astrocytes and microglia express a variety of adrenergic receptors [8,9], and astrocytes are particularly rich in  $\alpha$ 2a-ARs [10], and our unpublished results], the contributions of these receptors remain to be clarified. Interestingly, the expression pattern of adrenergic receptors is dynamically regulated depending on the physiological or pathological state of neurons and glia. For example, treatment of microglia with lipopolysaccharides (LPS) leads to a decrease in the expression of  $\beta$ 2-AR and upregulation of  $\alpha$ 2a-AR, which has a higher affinity for NA [9,25]. Therefore, it will be of value in future experiments to study the dynamic interplay between the expression and function of diverse noradrenergic receptors in chronic pain conditions and utilize these data to design novel receptor-specific therapies that could be used complementary to SNRIs. Finally, only at 21 days after nerve injury, we observed sexual dimorphism in the action of microglia and astrocytes, and effects of  $\beta$ 2-AR activation at early and late stages also hold implications for the choice of drugs and the optimal time frame of their use in therapy of neuropathic pain.

It is interesting to consider how microglia are affected by  $\beta$ 2-AR activation while suppressing neuropathic allodynia. In various pathological models, such as Alzheimer's or Parkinson's, the application of norepinephrine has been shown to have an anti-inflammatory effect, while the blockade of  $\beta$ 2-AR receptors by  $\beta$ -blockers promotes inflammation [48]. Furthermore,  $\beta$ 2-AR agonists have been shown to suppress inflammatory phenotypic changes in activated macrophages and microglia through activation of the cyclic AMP-protein kinase A (cAMP-PKA) pathway, suppression of the production of pro-inflammatory molecules such as TNF $\alpha$  and IL-1 $\beta$  [49,50], and by promoting the release of anti-inflammatory substances [51,52].  $\beta$ 2-AR agonists were also reported to promote the conversion of LPS-activated microglia from an M1- to M2-like phenotype via the classical cAMP/PKA/cAMP response element-binding protein (CREB) pathway, as well as via phosphoinositide 3-kinase (PI3K) and p38 MAPK signaling [53]. Similarly, several other studies report that modulating the astrocytic  $\beta$ 2-AR tone alters nuclear factor kappa-light-chain-enhancer of activated B cells (NF- $\kappa$ B)-dependent effects and the immune cell content of the CNS in pro-inflammatory conditions [54]. Taken together, previous studies and our data support that the anti-allodynic actions of  $\beta$ 2-AR, acting via microglia and astrocytes, can likely be attributed to the ability to hinder inflammatory crosstalk between neurons, glia and other immune cells in neuroinflammation after nerve injury.

Lately, the scientific community has shown vast interest in determining the influence of sex differences in the role of microglia in hypersensitivity [55,56]. Experiments in female mice that targeted the P2X4-BDNF-TRKB pathway and activation of p38 mitogen-activated protein kinase (MAPK) were ineffective in reducing pain hypersensitivity [57,58]. Nevertheless, numerous studies report no evident sexual dimorphism in the analgesic effect of microglial inhibitors, genetic knockout of microglial-selective molecules, or the ablation



of microglia in various nerve injury models [59–63]. Our results show that microgliosis (increased density, morphology shifting to an amoeboid phenotype, and upregulation of activation markers) is equally present in the SDH of both male and female mice three and six days after SNI and that Formoterol markedly lessens this aberrant upregulation. Regarding sex-specific changes, we found only a small number of notable differences in our behavior experiments. In the CPP test for spontaneous pain, soon after nerve injury, SNI-operated female mice do not show a significant preference towards the Formoterol-associated chamber, but only a trend. This indicates that a few days after nerve injury, the  $\beta$ 2-AR agonist analgesic effect in female mice is not as efficacious in reducing spontaneous pain as in male mice. The most striking difference appears to be the differential involvement of microglia 21 days after the operation. In contrast with male mice, microglia do not accumulate in the SDH of SNI-operated female mice similar to the sham-operated ones. Moreover, only in female mice at a late time point, Formoterol treatment fails to reverse the SNI-induced microglial enlargement of the soma and the shrinking of the processes and does not reduce the p-JNK signal in microglia. We can speculate that in female mice the microglia neuroimmune response is attenuated from the third week post-SNI. This suggests that microglia three weeks after SNI return to the basal resting state as the sham condition, in which the Formoterol effect is attenuated.

Furthermore, previous studies showed sex-independent astroglial signaling in the spinal cord in neuropathic pain [18], whereas others showed sex-dependent astrocytic response/uptake of glutamate and response to fatty acids in response to a brain injury [64]. In our study, Formoterol administration decreases p-JNK levels in astrocytes in the SDH of SNI-operated female mice but failed in male mice.

Finally, the observations of this study and previous studies on sexual dimorphism in the involvement of microglia and astrocytes [18,56] and the effects of  $\beta$ 2-AR activation at early and late stages also hold implications for the development of more target-specific drugs and the choice of the optimal time frame of their use in therapy of neuropathic pain.

**Supplementary Materials:** The following supporting information can be downloaded at: <https://www.mdpi.com/article/10.3390/cells12020284/s1>, Figure S1: SNI does not affect *Adrb2* mRNA expression in the spinal dorsal horn.  $\beta$ 2-AR agonist attenuates inflammatory cytokines release from activated primary microglia and modulates spared nerve injury-induced sensitization in a time-dependent manner. Figure S2: Formoterol attenuates mechanical hypersensitivity in SNI-operated mice. Temporal scheme of conditional place preference (CPP) and female mice CPP heatmaps. Figure S3: Response of SNI-operated mice to a single late injection of Formoterol. Figure S4: Formoterol effect on microglia in the spinal dorsal horn of sham-operated mice and negative controls for secondary antibodies.

**Author Contributions:** This work was conceived by M.S., A.A. and E.D.; data were collected and analyzed by E.D. and M.S.; the manuscript was written by M.S., E.D. and A.A. All authors have read and agreed to the published version of the manuscript.

**Funding:** This work was supported by the Deutsche Forschungsgemeinschaft in the form of an SFB1158 grant (Project A09 to A.A. and M.S.). M.S. is the recipient of the Olympia Morata Fellowship of Heidelberg University, and A.A. was supported in part by the Chica and Heinz Schaller Research Foundation. The data storage service (SDS@hd) is supported by the Ministry of Science, Research and the Arts Baden-Württemberg (MWK) and the German Research Foundation (DFG) through grant INST 35/1314-1 FUGG and INST 35/1503-1 FUGG.

**Institutional Review Board Statement:** All experimental procedures were approved by the local governing body (Regierungspräsidium Karlsruhe, Germany, Ref. 35-9185.81/G-177/17 and 35-9185.81/G-274/19) and abided by the German laws that regulate animal welfare and the protection of animals used for the scientific purpose (TierSchG, TierSchVersV).

**Informed Consent Statement:** Not applicable.

**Data Availability Statement:** The data presented in this study are openly available upon reasonable request.

**Acknowledgments:** The authors are grateful to C. Gartner for secretarial assistance, D. Baumgartl-Ahlert, T. Roth, and L.S. Grams for excellent technical assistance, R. Kuner (Pharmacology Institute, University of Heidelberg) for intellectual input and the help in writing the initial draft. We thank Frank Kirchhoff (CIPMM, Homburg, Saarland, Germany) for intellectual input and fruitful discussions. We further thank F. Kirchhoff (CIPMM, Homburg, Saarland, Germany), S. Jung (The Weizmann Institute of Science, Rehovot, Israel, and G. Karsenty (Columbia University, New York, NY, USA) for the *Cx3cr1-creERT2* and *Adrb2<sup>fl/fl</sup>* mice donation, respectively. Graphical abstract created with BioRender.com (<https://app.biorender.com/illustrations/63501b4ae31c8ffa17e5055e19/10/2022>). The authors gratefully acknowledge the Interdisciplinary Neurobehavioral Core Facility of Medical Faculty Heidelberg for assistance with behavioral experiments and the data storage service (SDS@hd).

**Conflicts of Interest:** M.S. is a guest editor for the special issue “Cellular and Molecular Mechanisms Underlying Pain Chronicity” at Cells. The funders had no role in the design of the study; in the collection, analyses, or interpretation of data; in the writing of the manuscript; or in the decision to publish the results.

## References

1. Finnerup, N.B.; Kuner, R.; Jensen, T.S. Neuropathic Pain: From Mechanisms to Treatment. *Physiol. Rev.* **2021**, *101*, 259–301. [[CrossRef](#)] [[PubMed](#)]
2. Finnerup, N.B.; Attal, N.; Haroutounian, S.; McNicol, E.; Baron, R.; Dworkin, R.H.; Gilron, I.; Haanpää, M.; Hansson, P.; Jensen, T.S.; et al. Pharmacotherapy for neuropathic pain in adults: A systematic review and meta-analysis. *Lancet Neurol.* **2015**, *14*, 162–173. [[CrossRef](#)] [[PubMed](#)]
3. Caraci, F.; Merlo, S.; Drago, F.; Caruso, G.; Parenti, C.; Sortino, M.A. Rescue of Noradrenergic System as a Novel Pharmacological Strategy in the Treatment of Chronic Pain: Focus on Microglia Activation. *Front. Pharmacol.* **2019**, *10*, 1024. [[CrossRef](#)] [[PubMed](#)]
4. Bahari, Z.; Meftahi, G.H. Spinal alpha2 -adrenoceptors and neuropathic pain modulation; therapeutic target. *Br. J. Pharmacol.* **2019**, *176*, 2366–2381. [[CrossRef](#)]
5. Fricker, L.D.; Margolis, E.B.; Gomes, I.; Devi, L.A. Five Decades of Research on Opioid Peptides: Current Knowledge and Unanswered Questions. *Mol. Pharmacol.* **2020**, *98*, 96–108. [[CrossRef](#)]
6. Pan, H.L.; Wu, Z.Z.; Zhou, H.Y.; Chen, S.R.; Zhang, H.M.; Li, D.P. Modulation of Pain Transmission by G Protein-Coupled Receptors. *Pharmacol. Ther.* **2008**, *117*, 141–161. [[CrossRef](#)]
7. Liu, B.; Eisenach, J.C. Hyperexcitability of axotomized and neighboring unaxotomized sensory neurons is reduced days after perineural clonidine at the site of injury. *J. Neurophysiol.* **2005**, *94*, 3159–3167. [[CrossRef](#)]
8. Zhang, X.; Wang, J.; Qian, W.; Zhao, J.; Sun, L.; Qian, Y.; Xiao, H. Dexmedetomidine inhibits tumor necrosis factor-alpha and interleukin 6 in lipopolysaccharide-stimulated astrocytes by suppression of c-Jun N-terminal kinases. *Inflammation* **2014**, *37*, 942–949. [[CrossRef](#)]
9. Ishii, Y.; Yamaizumi, A.; Kawakami, A.; Islam, A.; Choudhury, M.E.; Takahashi, H.; Yano, H.; Tanaka, J. Anti-inflammatory effects of noradrenaline on LPS-treated microglial cells: Suppression of NFκB nuclear translocation and subsequent STAT1 phosphorylation. *Neurochem. Int.* **2015**, *90*, 56–66. [[CrossRef](#)]
10. Kremer, M.; Salvat, E.; Muller, A.; Yalcin, I.; Barrot, M. Antidepressants and gabapentinoids in neuropathic pain: Mechanistic insights. *Neuroscience* **2016**, *338*, 183–206. [[CrossRef](#)]
11. Old, E.A.; Clark, A.K.; Malcangio, M. The role of glia in the spinal cord in neuropathic and inflammatory pain. *Handb. Exp. Pharmacol.* **2015**, *227*, 145–170. [[CrossRef](#)] [[PubMed](#)]
12. Donnelly, C.R.; Andriessen, A.S.; Chen, G.; Wang, K.; Jiang, C.; Maixner, W.; Ji, R.R. Central Nervous System Targets: Glial Cell Mechanisms in Chronic Pain. *Neurotherapeutics* **2020**, *17*, 846–860. [[CrossRef](#)] [[PubMed](#)]
13. Taves, S.; Berta, T.; Chen, G.; Ji, R.R. Microglia and spinal cord synaptic plasticity in persistent pain. *Neural. Plast.* **2013**, *2013*, 753656. [[CrossRef](#)]
14. Hald, A.; Nedergaard, S.; Hansen, R.R.; Ding, M.; Heegaard, A.M. Differential activation of spinal cord glial cells in murine models of neuropathic and cancer pain. *Eur. J. Pain* **2009**, *13*, 138–145. [[CrossRef](#)]
15. Gwak, Y.S.; Kang, J.; Unabia, G.C.; Hulsebosch, C.E. Spatial and temporal activation of spinal glial cells: Role of gliopathy in central neuropathic pain following spinal cord injury in rats. *Exp. Neurol.* **2012**, *234*, 362–372. [[CrossRef](#)]
16. Nam, Y.; Kim, J.H.; Kim, J.H.; Jha, M.K.; Jung, J.Y.; Lee, M.G.; Choi, I.S.; Jang, I.S.; Lim, D.G.; Hwang, S.H.; et al. Reversible Induction of Pain Hypersensitivity following Optogenetic Stimulation of Spinal Astrocytes. *Cell Rep.* **2016**, *17*, 3049–3061. [[CrossRef](#)] [[PubMed](#)]
17. Guan, Z.; Kuhn, J.A.; Wang, X.; Colquitt, B.; Solorzano, C.; Vaman, S.; Guan, A.K.; Evans-Reinsch, Z.; Braz, J.; Devor, M.; et al. Injured sensory neuron-derived CSF1 induces microglial proliferation and DAP12-dependent pain. *Nat. Neurosci.* **2016**, *19*, 94–101. [[CrossRef](#)]
18. Chen, G.; Zhang, Y.Q.; Qadri, Y.J.; Serhan, C.N.; Ji, R.R. Microglia in Pain: Detrimental and Protective Roles in Pathogenesis and Resolution of Pain. *Neuron* **2018**, *100*, 1292–1311. [[CrossRef](#)]

19. Lubahn, C.L.; Lorton, D.; Schaller, J.A.; Sweeney, S.J.; Bellinger, D.L. Targeting alpha- and beta-Adrenergic Receptors Differentially Shifts Th1, Th2, and Inflammatory Cytokine Profiles in Immune Organs to Attenuate Adjuvant Arthritis. *Front. Immunol.* **2014**, *5*, 346. [[CrossRef](#)]
20. Uzkeser, H.; Cadirci, E.; Halici, Z.; Odabasoglu, F.; Polat, B.; Yuksel, T.N.; Ozaltin, S.; Atalay, F. Anti-inflammatory and antinociceptive effects of salbutamol on acute and chronic models of inflammation in rats: Involvement of an antioxidant mechanism. *Mediat. Inflamm.* **2012**, *2012*, 438912. [[CrossRef](#)]
21. Zhang, F.F.; Morioka, N.; Abe, H.; Fujii, S.; Miyouchi, K.; Nakamura, Y.; Hisaoka-Nakashima, K.; Nakata, Y. Stimulation of spinal dorsal horn  $\beta$ 2-adrenergic receptor ameliorates neuropathic mechanical hypersensitivity through a reduction of phosphorylation of microglial p38 MAP kinase and astrocytic c-jun N-terminal kinase. *Neurochem. Int.* **2016**, *101*, 144–155. [[CrossRef](#)] [[PubMed](#)]
22. Arora, V.; Morado-Urbina, C.E.; Gwak, Y.S.; Parker, R.A.; Kittel, C.A.; Munoz-Islas, E.; Miguel Jimenez-Andrade, J.; Romero-Sandoval, E.A.; Eisenach, J.C.; Peters, C.M. Systemic administration of a beta2-adrenergic receptor agonist reduces mechanical allodynia and suppresses the immune response to surgery in a rat model of persistent post-incisional hypersensitivity. *Mol. Pain* **2021**, *17*, 1744806921997206. [[CrossRef](#)] [[PubMed](#)]
23. Albertini, G.; Etienne, F.; Roumier, A. Regulation of microglia by neuromodulators: Modulations in major and minor modes. *Neurosci. Lett.* **2020**, *733*, 135000. [[CrossRef](#)] [[PubMed](#)]
24. Zhang, Y.; Chen, K.; Sloan, S.A.; Bennett, M.L.; Scholze, A.R.; O’Keeffe, S.; Phatnani, H.P.; Guarnieri, P.; Caneda, C.; Ruderisch, N.; et al. An RNA-sequencing transcriptome and splicing database of glia, neurons, and vascular cells of the cerebral cortex. *J. Neurosci.* **2014**, *34*, 11929–11947. [[CrossRef](#)]
25. Gyoneva, S.; Traynelis, S.F. Norepinephrine modulates the motility of resting and activated microglia via different adrenergic receptors. *J. Biol. Chem.* **2013**, *288*, 15291–15302. [[CrossRef](#)]
26. Mori, K.; Ozaki, E.; Zhang, B.; Yang, L.; Yokoyama, A.; Takeda, I.; Maeda, N.; Sakanaka, M.; Tanaka, J. Effects of norepinephrine on rat cultured microglial cells that express alpha1, alpha2, beta1 and beta2 adrenergic receptors. *Neuropharmacology* **2002**, *43*, 1026–1034. [[CrossRef](#)]
27. Stowell, R.D.; Sipe, G.O.; Dawes, R.P.; Batchelor, H.N.; Lordy, K.A.; Whitelaw, B.S.; Stoessel, M.B.; Bidlack, J.M.; Brown, E.; Sur, M.; et al. Noradrenergic signaling in the wakeful state inhibits microglial surveillance and synaptic plasticity in the mouse visual cortex. *Nat. Neurosci.* **2019**, *22*, 1782–1792. [[CrossRef](#)]
28. Liu, Y.U.; Ying, Y.; Li, Y.; Eyo, U.B.; Chen, T.; Zheng, J.; Umpierre, A.D.; Zhu, J.; Bosco, D.B.; Dong, H.; et al. Neuronal network activity controls microglial process surveillance in awake mice via norepinephrine signaling. *Nat. Neurosci.* **2019**, *22*, 1771–1781. [[CrossRef](#)]
29. Hinoi, E.; Gao, N.; Jung, D.Y.; Yadav, V.; Yoshizawa, T.; Myers, M.G.; Chua, S.C.; Kim, J.K.; Kaestner, K.H.; Karsenty, G. The sympathetic tone mediates leptin’s inhibition of insulin secretion by modulating osteocalcin bioactivity. *J. Cell Biol.* **2008**, *183*, 1235–1242. [[CrossRef](#)] [[PubMed](#)]
30. Yona, S.; Kim, K.W.; Wolf, Y.; Mildner, A.; Varol, D.; Breker, M.; Strauss-Ayali, D.; Viukov, S.; Williams, M.; Misharin, A.; et al. Fate mapping reveals origins and dynamics of monocytes and tissue macrophages under homeostasis. *Immunity* **2013**, *38*, 79–91. [[CrossRef](#)]
31. Decosterd, I.; Woolf, C.J. Spared nerve injury: An animal model of persistent peripheral neuropathic pain. *Pain* **2000**, *87*, 149–158. [[CrossRef](#)]
32. Yalcin, I.; Tessier, L.H.; Petit-Demoulière, N.; Waltisperger, E.; Hein, L.; Freund-Mercier, M.J.; Barrot, M. Chronic treatment with agonists of beta(2)-adrenergic receptors in neuropathic pain. *Exp. Neurol.* **2010**, *221*, 115–121. [[CrossRef](#)] [[PubMed](#)]
33. Dixon, W.J. Efficient analysis of experimental observations. *Annu. Rev. Pharmacol. Toxicol.* **1980**, *20*, 441–462. [[CrossRef](#)]
34. Nees, T.A.; Wang, N.; Adamek, P.; Verkest, C.; La Porta, C.; Schaefer, I.; Virnich, J.; Balkaya, S.; Prato, V.; Morelli, C.; et al. The molecular mechanism and physiological role of silent nociceptor activation. *bioRxiv* **2022**. [[CrossRef](#)]
35. Huang, E.Y.; Liu, T.C.; Tao, P.L. Co-administration of dextromethorphan with morphine attenuates morphine rewarding effect and related dopamine releases at the nucleus accumbens. *Naunyn Schmiedeberg’s Arch. Pharmacol.* **2003**, *368*, 386–392. [[CrossRef](#)] [[PubMed](#)]
36. Schweizerhof, M.; Stösser, S.; Kurejova, M.; Njoo, C.; Gangadharan, V.; Agarwal, N.; Schmelz, M.; Bali, K.K.; Michalski, C.W.; Brugger, S.; et al. Hematopoietic colony-stimulating factors mediate tumor-nerve interactions and bone cancer pain. *Nat. Med.* **2009**, *15*, 802–807. [[CrossRef](#)]
37. Bohlen, C.J.; Bennett, F.C.; Tucker, A.F.; Collins, H.Y.; Mulinyawe, S.B.; Barres, B.A. Diverse Requirements for Microglial Survival, Specification, and Function Revealed by Defined-Medium Cultures. *Neuron* **2017**, *94*, 759–773.e758. [[CrossRef](#)]
38. Costigan, M.; Scholz, J.; Woolf, C.J. Neuropathic pain: A maladaptive response of the nervous system to damage. *Annu. Rev. Neurosci.* **2009**, *32*, 1–32. [[CrossRef](#)] [[PubMed](#)]
39. King, T.; Vera-Portocarrero, L.; Gutierrez, T.; Vanderah, T.W.; Dussor, G.; Lai, J.; Fields, H.L.; Porreca, F. Unmasking the tonic-aversive state in neuropathic pain. *Nat. Neurosci.* **2009**, *12*, 1364–1366. [[CrossRef](#)]
40. Pitzer, C.; Kuner, R.; Tappe-Theodor, A. EXPRESS: Voluntary and evoked behavioral correlates in neuropathic pain states under different housing conditions. *Mol. Pain* **2016**, *12*, 1744806916656635. [[CrossRef](#)]
41. Chen, Z.; Doyle, T.M.; Luongo, L.; Largent-Milnes, T.M.; Giancotti, L.A.; Kolar, G.; Squillace, S.; Boccella, S.; Walker, J.K.; Pendleton, A.; et al. Sphingosine-1-phosphate receptor 1 activation in astrocytes contributes to neuropathic pain. *Proc. Natl. Acad. Sci. USA* **2019**, *116*, 10557–10562. [[CrossRef](#)]

42. Ji, R.R.; Suter, M.R. p38 MAPK, microglial signaling, and neuropathic pain. *Mol. Pain* **2007**, *3*, 33. [[CrossRef](#)] [[PubMed](#)]
43. Kuner, R.; Flor, H. Structural plasticity and reorganisation in chronic pain. *Nat. Rev. Neurosci.* **2016**, *18*, 20–30. [[CrossRef](#)] [[PubMed](#)]
44. Ceredig, R.A.; Pierre, F.; Doridot, S.; Alduntzin, U.; Hener, P.; Salvat, E.; Yalcin, I.; Gaveriaux-Ruff, C.; Barrot, M.; Massotte, D. Peripheral Delta Opioid Receptors Mediate Formoterol Anti-allodynic Effect in a Mouse Model of Neuropathic Pain. *Front. Mol. Neurosci.* **2019**, *12*, 324. [[CrossRef](#)]
45. Kremer, M.; Megat, S.; Bohren, Y.; Wurtz, X.; Nexon, L.; Ceredig, R.A.; Doridot, S.; Massotte, D.; Salvat, E.; Yalcin, I.; et al. Delta opioid receptors are essential to the antiallodynic action of Beta2-mimetics in a model of neuropathic pain. *Mol. Pain* **2020**, *16*, 1744806920912931. [[CrossRef](#)] [[PubMed](#)]
46. Kremer, M.; Yalcin, I.; Goumon, Y.; Wurtz, X.; Nexon, L.; Daniel, D.; Megat, S.; Ceredig, R.A.; Ernst, C.; Turecki, G.; et al. A Dual Noradrenergic Mechanism for the Relief of Neuropathic Allodynia by the Antidepressant Drugs Duloxetine and Amitriptyline. *J. Neurosci.* **2018**, *38*, 9934–9954. [[CrossRef](#)] [[PubMed](#)]
47. Damo, E. Glial cells as target for antidepressants in neuropathic pain. *Neuroforum* **2022**, *28*, 85–94. [[CrossRef](#)]
48. Evans, A.K.; Ardestani, P.M.; Yi, B.; Park, H.H.; Lam, R.K.; Shamloo, M. Beta-adrenergic receptor antagonism is proinflammatory and exacerbates neuroinflammation in a mouse model of Alzheimer’s Disease. *Neurobiol. Dis.* **2020**, *146*, 105089. [[CrossRef](#)] [[PubMed](#)]
49. Izeboud, C.A.; Monshouwer, M.; van Miert, A.S.; Witkamp, R.F. The beta-adrenoceptor agonist clenbuterol is a potent inhibitor of the LPS-induced production of TNF-alpha and IL-6 in vitro and in vivo. *Inflamm. Res.* **1999**, *48*, 497–502. [[CrossRef](#)]
50. Keranen, T.; Hommo, T.; Moilanen, E.; Korhonen, R. beta2-receptor agonists salbutamol and terbutaline attenuated cytokine production by suppressing ERK pathway through cAMP in macrophages. *Cytokine* **2017**, *94*, 1–7. [[CrossRef](#)]
51. Agac, D.; Estrada, L.D.; Maples, R.; Hooper, L.V.; Farrar, J.D. The beta2-adrenergic receptor controls inflammation by driving rapid IL-10 secretion. *Brain Behav. Immun.* **2018**, *74*, 176–185. [[CrossRef](#)]
52. Keranen, T.; Hommo, T.; Hamalainen, M.; Moilanen, E.; Korhonen, R. Anti-Inflammatory Effects of beta2-Receptor Agonists Salbutamol and Terbutaline Are Mediated by MKP-1. *PLoS ONE* **2016**, *11*, e0148144. [[CrossRef](#)] [[PubMed](#)]
53. Sharma, M.; Arbabzada, N.; Flood, P.M. Mechanism underlying beta2-AR agonist-mediated phenotypic conversion of LPS-activated microglial cells. *J. Neuroimmunol.* **2019**, *332*, 37–48. [[CrossRef](#)] [[PubMed](#)]
54. Laureys, G.; Clinckers, R.; Gerlo, S.; Spooren, A.; Wilczak, N.; Kooijman, R.; Smolders, I.; Michotte, Y.; De Keyser, J. Astrocytic beta(2)-adrenergic receptors: From physiology to pathology. *Prog. Neurobiol.* **2010**, *91*, 189–199. [[CrossRef](#)] [[PubMed](#)]
55. Midavaine, E.; Cote, J.; Marchand, S.; Sarret, P. Glial and neuroimmune cell choreography in sexually dimorphic pain signaling. *Neurosci. Biobehav. Rev.* **2021**, *125*, 168–192. [[CrossRef](#)]
56. Mogil, J.S. Qualitative sex differences in pain processing: Emerging evidence of a biased literature. *Nat. Rev. Neurosci.* **2020**, *21*, 353–365. [[CrossRef](#)]
57. Taves, S.; Berta, T.; Liu, D.L.; Gan, S.; Chen, G.; Kim, Y.H.; Van de Ven, T.; Laufer, S.; Ji, R.R. Spinal inhibition of p38 MAP kinase reduces inflammatory and neuropathic pain in male but not female mice: Sex-dependent microglial signaling in the spinal cord. *Brain Behav. Immun.* **2016**, *55*, 70–81. [[CrossRef](#)]
58. Sorge, R.E.; Mapplebeck, J.C.; Rosen, S.; Beggs, S.; Taves, S.; Alexander, J.K.; Martin, L.J.; Austin, J.S.; Sotocinal, S.G.; Chen, D.; et al. Different immune cells mediate mechanical pain hypersensitivity in male and female mice. *Nat. Neurosci.* **2015**, *18*, 1081–1083. [[CrossRef](#)]
59. Batti, L.; Sundukova, M.; Murana, E.; Pimpinella, S.; De Castro Reis, F.; Pagani, F.; Wang, H.; Pellegrino, E.; Perlas, E.; Di Angelantonio, S.; et al. TMEM16F Regulates Spinal Microglial Function in Neuropathic Pain States. *Cell Rep.* **2016**, *15*, 2608–2615. [[CrossRef](#)]
60. Peng, J.; Gu, N.; Zhou, L.; B Eyo, U.; Murugan, M.; Gan, W.B.; Wu, L.J. Microglia and monocytes synergistically promote the transition from acute to chronic pain after nerve injury. *Nat. Commun.* **2016**, *7*, 12029. [[CrossRef](#)]
61. Gu, N.; Eyo, U.B.; Murugan, M.; Peng, J.; Matta, S.; Dong, H.; Wu, L.J. Microglial P2Y12 receptors regulate microglial activation and surveillance during neuropathic pain. *Brain. Behav. Immun.* **2016**, *55*, 82–92. [[CrossRef](#)] [[PubMed](#)]
62. Staniland, A.A.; Clark, A.K.; Wodarski, R.; Sasso, O.; Maione, F.; D’Acquisto, F.; Malcangio, M. Reduced inflammatory and neuropathic pain and decreased spinal microglial response in fractalkine receptor (CX3CR1) knockout mice. *J. Neurochem.* **2010**, *114*, 1143–1157. [[CrossRef](#)] [[PubMed](#)]
63. Barragan-Iglesias, P.; Pineda-Farias, J.B.; Cervantes-Duran, C.; Bravo-Hernandez, M.; Rocha-Gonzalez, H.I.; Murbartian, J.; Granados-Soto, V. Role of spinal P2Y6 and P2Y11 receptors in neuropathic pain in rats: Possible involvement of glial cells. *Mol. Pain* **2014**, *10*, 29. [[CrossRef](#)] [[PubMed](#)]
64. Crespo-Castrillo, A.; Arevalo, M.A. Microglial and Astrocytic Function in Physiological and Pathological Conditions: Estrogenic Modulation. *Int. J. Mol. Sci.* **2020**, *21*, 3219. [[CrossRef](#)]

**Disclaimer/Publisher’s Note:** The statements, opinions and data contained in all publications are solely those of the individual author(s) and contributor(s) and not of MDPI and/or the editor(s). MDPI and/or the editor(s) disclaim responsibility for any injury to people or property resulting from any ideas, methods, instructions or products referred to in the content.